
# NAVAL POSTGRADUATE SCHOOL

**MONTEREY, CALIFORNIA**

# THESIS

**VARIABILITY IN GLOBAL-SCALE CIRCULATIONS AND THEIR IMPACTS ON ATLANTIC TROPICAL CYCLONE ACTIVITY**

by

Matthew J. Rosencrans

June 2006

| | |
|---|---|
| Thesis Advisor: | Patrick Harr |
| Co-Advisor: | Tom Murphree |

**Approved for public release; distribution is unlimited.**

THIS PAGE INTENTIONALLY LEFT BLANK

| REPORT DOCUMENTATION PAGE | | | Form Approved OMB No. 0704-0188 |
|---|---|---|---|
| Public reporting burden for this collection of information is estimated to average 1 hour per response, including the time for reviewing instruction, searching existing data sources, gathering and maintaining the data needed, and completing and reviewing the collection of information. Send comments regarding this burden estimate or any other aspect of this collection of information, including suggestions for reducing this burden, to Washington headquarters Services, Directorate for Information Operations and Reports, 1215 Jefferson Davis Highway, Suite 1204, Arlington, VA 22202-4302, and to the Office of Management and Budget, Paperwork Reduction Project (0704-0188) Washington DC 20503. | | | |
| **1. AGENCY USE ONLY** ***(Leave blank)*** | **2. REPORT DATE** June 2006 | **3. REPORT TYPE AND DATES COVERED** Master's Thesis | |
| **4. TITLE AND SUBTITLE:** Variability in Global-scale Circulations and Their Impacts on Atlantic Tropical Cyclone Activity. | | **5. FUNDING NUMBERS** | |
| **6. AUTHOR(S)** Matthew J. Rosencrans | | | |
| **7. PERFORMING ORGANIZATION NAME(S) AND ADDRESS(ES)** Naval Postgraduate School Monterey, CA 93943-5000 | | **8. PERFORMING ORGANIZATION REPORT NUMBER** | |
| **9. SPONSORING /MONITORING AGENCY NAME(S) AND ADDRESS(ES)** N/A | | **10. SPONSORING/MONITORING AGENCY REPORT NUMBER** | |
| **11. SUPPLEMENTARY NOTES** The views expressed in this thesis are those of the author and do not reflect the official policy or position of the Department of Defense or the U.S. Government. | | | |
| **12a. DISTRIBUTION / AVAILABILITY STATEMENT** Approved for public release; distribution is unlimited. | | **12b. DISTRIBUTION CODE** A | |


**13. ABSTRACT (maximum 200 words)**

In this study, intraseasonal variations in Southern Hemisphere midlatitude large-scale circulations are examined with respect to environmental factors over the tropical North Atlantic that may be favorable or unfavorable for tropical cyclone formation. Favorable impacts on tropical Atlantic circulation characteristics are defined by an increase in low-level relative vorticity, a decrease in westerly vertical wind shear, and increased convection in the West African monsoon (WAM).

The second and third modes of an empirical orthogonal function (EOF) analysis of the 700-hPa height anomalies identify a distinct Rossby-wave pattern. Significant variability in the Southern Hemisphere mid-latitude circulations is related to the two EOF modes and to equatorward Rossby-wave dispersion.

Formation of a large cyclonic anomaly over the southeast Pacific, west of Chile, is related to equatorward propagation of a Rossby-like wave across South America, toward the equatorial Atlantic. The cyclonic anomaly precedes an increase in WAM convection by an average of two days, which then precedes westerly wind anomalies over the equatorial North Atlantic by several days. Tropical cyclone formation is found to be enhanced when the increased equatorial westerly anomalies coincide with reduced vertical wind shear, which is related to Northern Hemisphere midlatitude circulations.


| **14. SUBJECT TERMS** Southern Hemisphere Midlatitudes, Rossby-Wave Dispersion, Large-scale Tropical Circulations, Intraseasonal Variability, Tropical Cyclones, Tropical North Atlantic, Antarctic Oscillation | | | **15. NUMBER OF PAGES** 99 |
|---|---|---|---|
| | | | **16. PRICE CODE** |
| **17. SECURITY CLASSIFICATION OF REPORT** Unclassified | **18. SECURITY CLASSIFICATION OF THIS PAGE** Unclassified | **19. SECURITY CLASSIFICATION OF ABSTRACT** Unclassified | **20. LIMITATION OF ABSTRACT** UL |

NSN 7540-01-280-5500

Standard Form 298 (Rev. 2-89)
Prescribed by ANSI Std. 239-18

THIS PAGE INTENTIONALLY LEFT BLANK

**Approved for public release; distribution is unlimited.**

**VARIABILITY IN GLOBAL-SCALE CIRCULATIONS AND THEIR IMPACTS ON ATLANTIC TROPICAL CYCLONE ACTIVITY**

Matthew J. Rosencrans
Captain, United States Air Force
B.S., University at Albany-State University of New York, 2001

Submitted in partial fulfillment of the
requirements for the degree of

**MASTER OF SCIENCE IN METEOROLOGY**

from the

**NAVAL POSTGRADUATE SCHOOL**
**June 2006**

Author: Matthew J. Rosencrans

Approved by: Patrick Harr
Thesis Advisor

Tom Murphree
Co-Advisor

Philip A. Durkee
Chairman, Department of Meteorology

THIS PAGE INTENTIONALLY LEFT BLANK

# ABSTRACT

In this study, intraseasonal variations in Southern Hemisphere midlatitude large-scale circulations are examined with respect to environmental factors over the tropical North Atlantic that may be favorable or unfavorable for tropical cyclone formation. Favorable impacts on tropical Atlantic circulation characteristics are defined by an increase in low-level relative vorticity, a decrease in westerly vertical wind shear, and increased convection in the West African monsoon (WAM).

The second and third modes of an empirical orthogonal function (EOF) analysis of the 700-hPa height anomalies identify a distinct Rossby-wave pattern. Significant variability in the Southern Hemisphere mid-latitude circulations is related to the two EOF modes and to equatorward Rossby-wave dispersion.

Formation of a large cyclonic anomaly over the southeast Pacific, west of Chile, is related to equatorward propagation of a Rossby-like wave across South America, toward the equatorial Atlantic. The cyclonic anomaly precedes an increase in WAM convection by an average of two days, which then precedes westerly wind anomalies over the equatorial North Atlantic by several days. Tropical cyclone formation is found to be enhanced when the increased equatorial westerly anomalies coincide with reduced vertical wind shear, which is related to Northern Hemisphere midlatitude circulations.

THIS PAGE INTENTIONALLY LEFT BLANK

# TABLE OF CONTENTS

# LIST OF FIGURES

# LIST OF TABLES

THIS PAGE INTENTIONALLY LEFT BLANK

# ACKNOWLEDGMENTS

I would like to thank Professor Patrick Harr for his ceaseless dedication and everlasting patience. Your guidance, vision, and leadership were instrumental to the successful completion of this work. Thank you for helping to illustrate how ones personal interests can be combined with scientific methods to result in great achievements. I wish you the best of luck in your future endeavors.

I would also like to thank Professor Tom Murphree for his continued guidance. Your insights were both inspirational and educational. The passion you possess for your field is remarkable; it inspires us all to push a little further, while keeping the basics in the forefronts of our minds.

To the other faculty and staff that have guided, instructed and mentored me along the path, you have my sincerest thanks. The level of dedication to the success of each and every student that you exhibit is unparalleled.

To my parents, thanks for always being there to guide me down the right path. Without your efforts, none of this would be possible.

THIS PAGE INTENTIONALLY LEFT BLANK

# I. INTRODUCTION

## A. OBJECTIVE

The significant influence that the weather exerts on military operations has been recognized and analyzed for thousands of years. Since the 6th century B.C., military strategists have been studying the works of Sun Tzu, who labeled the heavens [in reference to the surrounding environmental conditions] as one of the five "matters" that every successful military leader will come to know in great depth. It was even hypothesized that consistently going against the weather will in itself lead to defeat, regardless of what preparations were made by the warring factions (McNeilly 2001). This concept was recently restated as, "Neglected or ignored, terrestrial and space weather and its effects can doom even the most carefully planned and executed campaigns and operations." (HQ USAF/XOO-W 2005).

In addition to directly influencing kinetic operations, such as a missile strike, atmospheric conditions play a significant role in non-kinetic warfare, which encompasses the traditional role of natural disaster response. Using non-kinetic means, such as delivering food aid, significant battles can be won before the first shot is even fired. Dr. Thomas P.M. Barnett has stated, "We respond to natural disaster simply to win wars without firing shots." Responding to natural disasters can win over the hearts and minds of a people, before they have the desire to bear arms. Therefore, knowing when and where a natural disaster is likely to occur can further the national interests of the United States and abate the need for traditional kinetic operations. Stated succinctly, "less Clausewitz; more Sun Tzu". (Barnett 2006, personal communication). Hence, knowing the weather is critical to the overall success of a mission and even to the reduction of conflict in general.

The fact that significant environmental events, such as drought, floods, or hurricanes, can adversely affect U.S. national or regional security without even involving opposing forces is a key driving factor behind the need to improve our

ability to forecast these events (Demmert et al. 2005). The joint U.S. meteorological and oceanographic (METOC) community recognized this and expressed an explicit interest in improving long-range forecasting capabilities to enable the U.S. government to better respond to environmental crises. The Air Force Weather Strategic Plan and Vision (2004) goes on to define the ability to predict and exploit meteorological impacts to military operations on extended time scales as a core process for the METOC community.

To assess the current impacts, current shortfalls, and future direction of weather operations, the Air Force Weather Agency (AFWA) has recently evaluated the impact of weather services to combatant commands. The concept of environmental security as placed in the combatant command level is rather new, and needs attention. Demmert et al. (2005) noted that the combatant commands call for skillful, longer-range, multidimensional forecasts. Demmert et al. (2005) go on to explicitly define longer-range range forecasts as those beyond 240h.

The U.S. government has an inherent requirement to respond to environmental crises worldwide, and even more so in developing nations, what Barnett (2004) terms the “Non-Integrated Gap”, as illustrated in Figure 1.1. Most of the “Non-Integrated Gap” lies in what is traditionally defined as the tropics (Riehl 1954). Combining that fact, with the testimonial that forecasts for timescales longer than 240h still provide a unique challenge for the DoD (HQ USAF/XOO-W 2005), the need to be able to more accurately predict tropical cyclone (TC) activity at longer time-scales becomes obvious.

The objective of this study is to investigate the impact of global-scale circulations, predominately Southern Hemisphere (SH) mid-latitude variability, on factors in large-scale atmospheric circulations that have been shown to modulate TC activity in the tropical North Atlantic during the boreal summer. The primary factors of atmospheric variability in the tropical North Atlantic are westward moving synoptic-scale waves that form over West Africa and then over the tropical Atlantic Ocean. The primary SH features of interest are circulations that

act to increase the background vorticity across the tropical North Atlantic. This would provide a favorable environment for wave growth in this region. Another major circulation influence on the African wave activity is the propagation of large-scale atmospheric circulations over the region of the West African monsoon. Therefore, an active monsoon may provide favorable conditions for wave growth. The SH and West African circulations are discussed below.

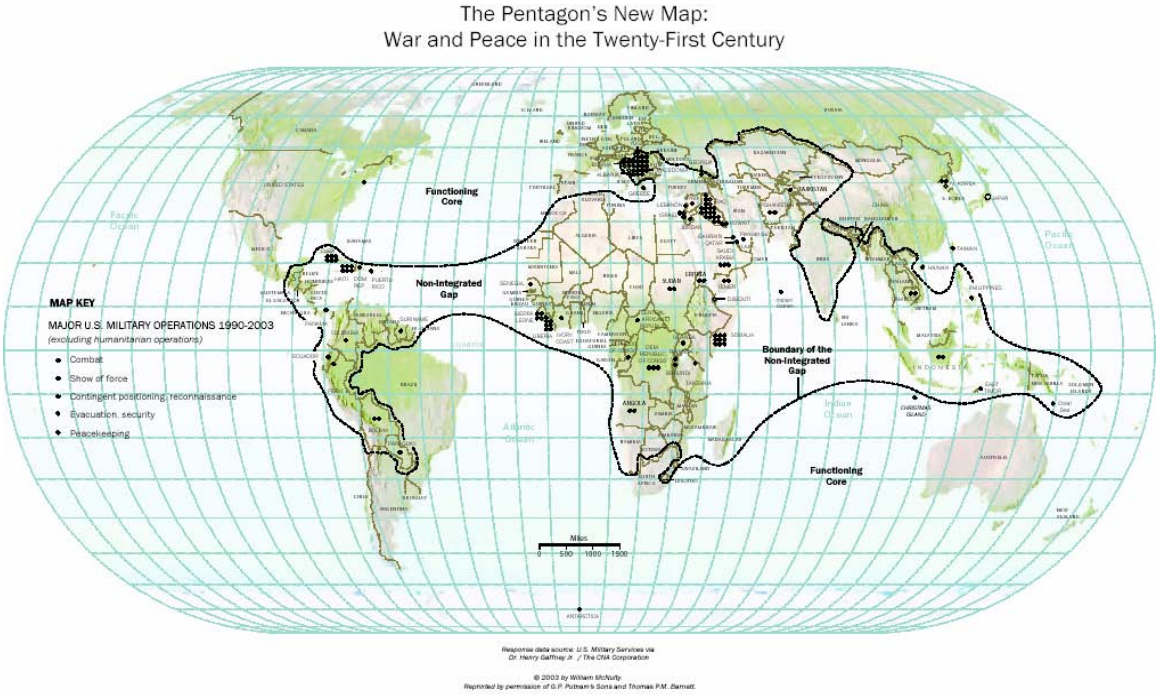


Figure 1.1 Map depicting locations of U.S. military operations during 1990-2003. Heavy line represents the division between the "Functioning Core" and "Non-Integrated Gap" (From Barnett 2004).

## B. BACKGROUND

### 1. Southern Hemisphere/ Western North Pacific Connection

Burton (2005) identified a significant connection between SH mid-latitude circulations and convective activity in the western North Pacific monsoon trough during the Northern Hemisphere (NH) summer. The mid-latitude variations and tropical circulations anomalies that support anomalous convection in the western North Pacific monsoon trough were found to have statistically significant variance in the 15 – 25 day time period. Using empirical orthogonal function (EOF)

analysis of time filtered, 700-hPa height anomalies over the SH, Burton (2005) identified vacillations in the SH height field and associated jet stream that led to equatorward propagation of wave energy. To remain consistent with previous studies, the leading mode of the EOF analysis was used by Burton (2005) to define the Antarctic Oscillation (AAO). The connection between the western North Pacific variations and SH mid-latitude fluctuations, as measured by a change in sign of the AAO index, was established by examining periods of wave activity in the western North Pacific monsoon trough and concurrent periods of transition in the phase of the AAO (Burton 2005).

Burton (2005) also presented modes two and three (Figures 1.2 and 1.3), which appear to represent a Rossby-wave train with a zonal wavenumber three structure. This structure was defined by the near quadrature phase relationship of these two modes, and the close relation in explained variance. These results were similar to those presented in Kiladis and Mo (1988).

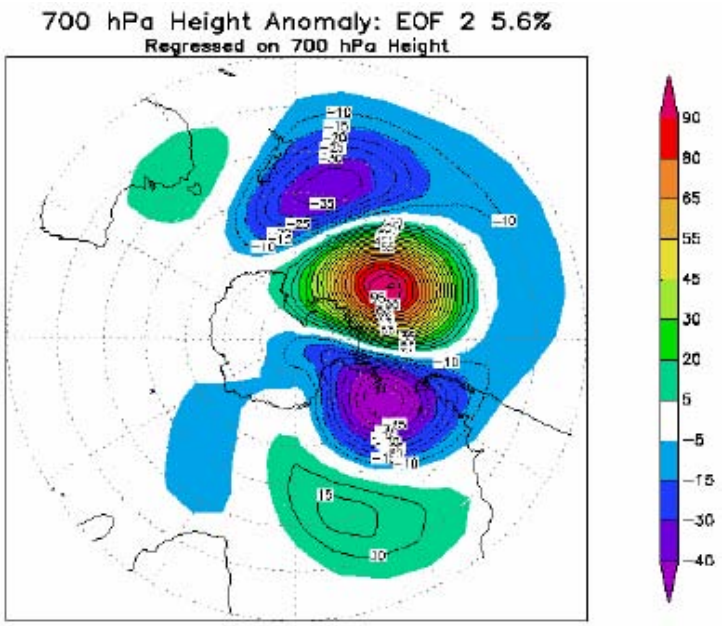


Figure 1.2 700-hPa height anomalies (m) from 1979-2003 regressed onto the second EOF pattern of 700-hPa heights. Contour interval is 5 m. Negative contours are dashed (From Burton 2005).

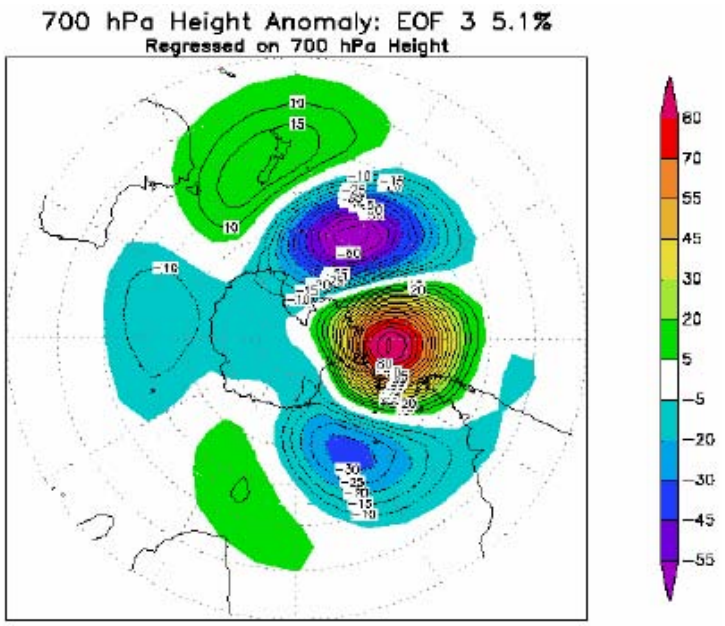


Figure 1.3 As in Figure 1.2 except for the third EOF pattern of 700-hPa heights (From Burton 2005).

Mo and Paegle (2001) presented similar EOF analysis results of 500-hPa height anomalies over the SH. Their EOF 2 defined the Pacific-South American mode 1 (PSA 1) and their EOF 3 pattern defined PSA 2. The structures of PSA 1 and PSA 2 were similar to modes 2 and 3 of the EOF analysis presented by Burton (2005). Over intraseasonal time scales, Mo and Paegle (2001) linked PSA 2 to tropical convection related to the Madden-Julian Oscillation (MJO) and also described its variability with respect to a 22-day period.

Burton (2005) identified a relationship between the state of the AAO and active periods of convection in the western North Pacific monsoon trough as identified by Delk (2004). The nature of the relationship was such that the transitions between phases of the AAO had the most significant impact on the anomalous wave structure in the Eastern Hemisphere. A shift in the AAO from negative to positive often resulted in a peak AAO value that coincided with an increase in low-level westerlies on the equatorial side of the NH monsoon trough. This transition was often associated with enhanced equatorial convection

(Figure 1.4). The reverse case (Figure 1.4 bottom), was a transition in the AAO from positive to negative, which led to suppressed convection in the monsoon trough.

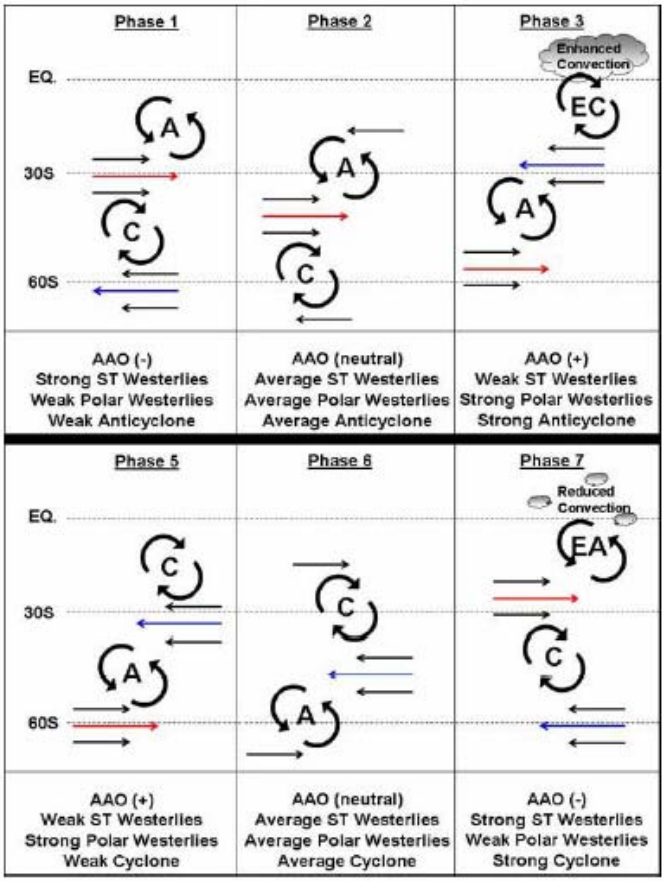


Figure 1.4 Schematic of anomalous wave activity in the Southern Hemisphere related to the AAO transition from a negative to positive index (top) during phases 1-3 of the 15- to 25-day cycle and from a positive to negative index (bottom) during phases 5-7 of the 15- to 25-day cycle. Vector lengths indicate strength of the anomalous zonal winds (From Burton 2005).

### 2. Atlantic/West African Monsoon

Whereas Delk (2004) identified significant links between regional wind patterns and regional rainfall patterns over the tropical North Pacific on intraseasonal timescales, Sultan et al. (2003) identified a significant link between specific low-level wind patterns and regional rainfall patterns on the intraseasonal timescale in the Western African monsoon (WAM) and the equatorial Atlantic. Sultan et al. (2003) linked 10-25 day filtered rainfall anomalies with significant

925-hPa circulation anomalies in the eastern Atlantic and Gulf of Guinea. The composite charts (Figure 1.5) define an approximately 15 day cycle in the circulation/rainfall coupled pattern.

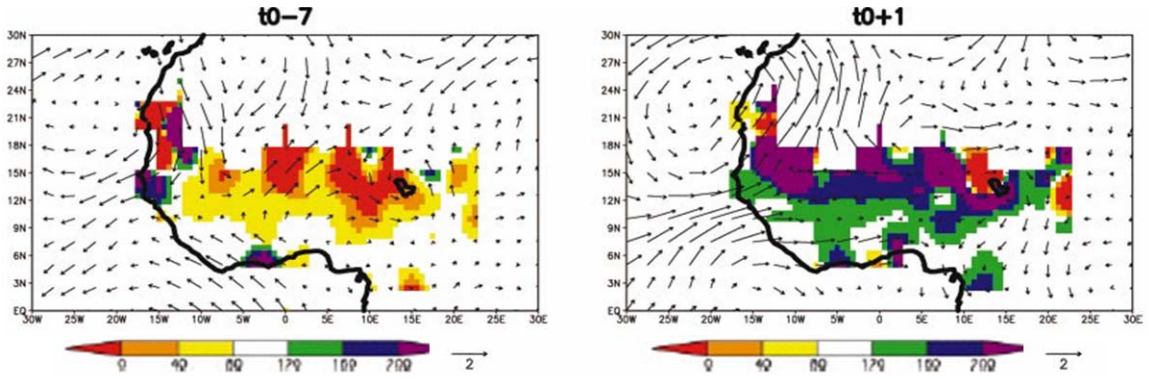


Figure 1.5 The composite 1968–90 wet–dry time sequence of the unfiltered rainfall field (colors) and the 925-hPa wind field (vector) from $t_0$-7 days to $t_0$+7 days by a step of 2 days, where $t_o$ defines the day of peak rainfall. Wet (dry) sequences are selected when the 10–25-day filtered regional rainfall index is max (min) and greater (less) than 30% of the seasonal-filtered rainfall signal. The rainfall values displayed in the figure (shaded according to the color bar below each panel) are the ratio of the daily unfiltered rainfall to the seasonal-filtered rainfall signal. They are expressed in percentages of the seasonal timescale signal and displayed for values lower than 80% and greater than 120%. The corresponding composite 925-hPa wind field is computed as the unfiltered wind difference between the wet and the dry sequences. Reference vectors for the winds (m $s^{-1}$) are displayed in the bottom right of each figure. (Adapted from Sultan et al. 2003)

The relationship between 925-hPa circulation anomalies and outgoing longwave radiation (OLR) (Figure 1.6), which was used as a proxy for convection, was further evidence of a basin wide relationship between these anomalous circulations (Sultan et al 2003). In the OLR composites, it can be seen that the convection associated with the WAM is related to an onshore component of the flow over West Africa, and that the zonal wind in the equatorial Atlantic is linked to distinct circulations in both the NH and SH. The two cyclonic circulations that straddle the equator in the right panel of Figure 1.6 act to increase equatorial westerlies, which have been positively correlated with the potential for TC development in the region (DeMaria 1999). Grodsky and Carton (2001) have also studied the relationship between winds and precipitation/OLR

on the intraseasonal time scale over West Africa. Their study confirmed the presence of a quasi-biweekly oscillation in the WAM circulation system. Sultan et al. (2003) also stated, “The role of atmospheric interactions from midlatitudes in the initiation of these intraseasonal timescale sequences over West Africa should be considered…”

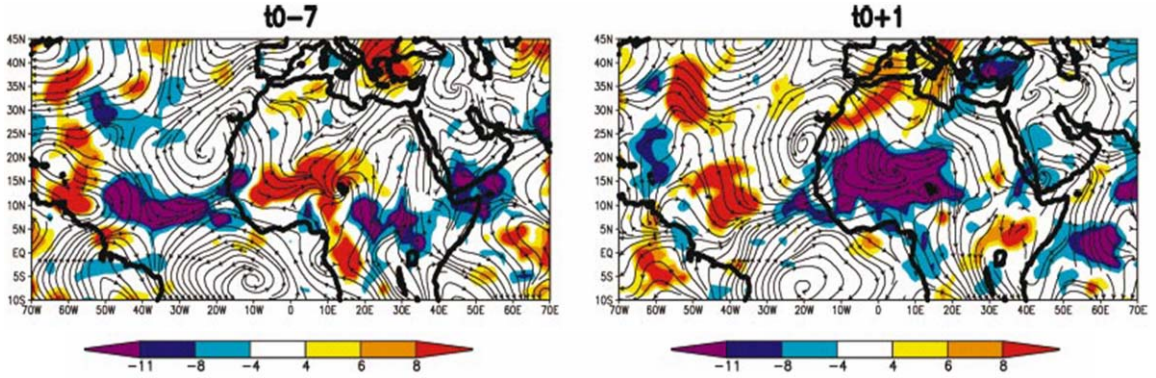


Figure 1.6 As in Figure 1.5 but for OLR values instead of rainfall values, and displayed on a wider domain. In this figure, the 925-hPa wind fields are displayed by streamlines and have been computed using a 3-day moving average to get a bit smoother field for better clarity. The composite OLR sequence has been computed from the available period 1979–90 and the composite wind sequence from the period 1968–90. OLR values (W $m^{-2}$) are the unfiltered value differences between wet and dry sequences, and not expressed in percentages as it is done for rainfall on Fig. 1.4 (Adapted from Sultan et al. 2003).

### 3. Extratropical-Tropical Interactions

Kiladis and Weickmann (1992b) related intraseasonal variability in convective activity over the northern portions of South America in the Atlantic Intertropical Convergence Zone (ITCZ) during the NH winter to the equatorward propagation of midlatitude troughs from the NH. They also stated that South America is a region where disturbances in the westerlies act to force tropical convection, even though the westerlies do not extend completely to the equator. Through simulations with a global primitive equation model, Hoskins and Yang (2000) showed that when westerlies occur close to equatorial regions, a response to a midlatitude forcing is possible. Through simulations with a barotropic model, Ambrizzi et al. (1995) further showed that there is a preferred path for Rossby-wave propagation out of the SH midlatitudes that heads toward

to the South Atlantic and eventually terminates in the equatorial South Atlantic. The combination of a preferred path for wave propagation into the area (Ambrizzi et al. 1995) with an area of mean westerlies during the northern summer lying close to the equator (Kiladis and Weickmann 1992b) provides motivation for the hypothesis in this study; significant low frequency atmospheric wave activity in the SH midlatitudes can force circulation changes in the equatorial Atlantic.

On intraseasonal timescales, downstream effects of waves that propagate along an arced path from the central South Pacific, through the southern portions of Chile and into the eastern regions of South American were described in both Mo and Paegle (2000) and Liebmann et al (1999). The studies employed different methods of analysis to derive similar results.

Mo and Paegle (2001) described significant downstream effects of PSA 1 and PSA 2 on rainfall over South America during the austral summer. A positive phase PSA 2 was linked to a northwest-southeast oriented region of decreased convective activity and precipitation in the South Atlantic Convergence Zone (SACZ) but increased precipitation in Argentina and Uruguay coastal regions. The composite of significant PSA 1 events identified a north-south dipole, with the anomalously dry conditions oriented east-west along the central Amazon region.

Liebmann et al. (1999) used linear regression to examine the relation of convection in the SACZ to large-scale atmospheric circulations on the submonthly timescale. Using 200-hPa streamfunction data that were filtered to remove fluctuations with periods longer than 30 days, Liebmann et al. (1999) showed that convection that moved into the SACZ from the southeast was linked to circulations that originated over the South Atlantic while convection that moved into the SACZ from the southwest was linked to midlatitude wave trains moving into the region from the central Pacific. The 200-hPa streamfunction associated with an OLR minimum at four days prior to the convective minimum is very similar to the pattern in EOF 2 of Burton (2005). Regardless of where the forcing for the convection in the SACZ originated, an anomalous, clockwise circulation

forms on the equator and spans the entire width of the Atlantic two days after the convective maximum in the SACZ. While Kiladis and Weickmann (1992b, 1997) attributed most of the variability in the Atlantic ITCZ during the boreal winter to trough intrusions from the midlatitudes, Liebmann et al, (1999) established the possibility that equatorward propagating features may account for another source of variability in the equatorial Atlantic during the northern summer.

## 4. Synopsis

The hypothesis for this study is that variations in the SH mid-latitudes propagate equatorward in the region of South America, and have a downstream impact on the large-scale flow and deep convection over the tropical North Atlantic and West Africa. The mid-latitude variations are related to the large-scale dynamics present in the South Pacific, which define the preferred wave-propagation path as approximately a great circle route around southernmost South America, and toward the equatorial Atlantic. The impacts on the large-scale circulation in the Atlantic are defined as those that influence low-level relative vorticity across the equatorial North Atlantic. Because the WAM is a known source of variability in the tropical North Atlantic that has a large affect on the regional wind patterns, wave activity and convective activity (Landsea and Gray 1992), the impact of the SH midlatitudes on the WAM is also investigated.

# II. DATA AND METHODOLOGY

## A. DATA

For this study, the 2.5° latitude by 2.5° longitude global, gridded reanalysis fields (Kalnay et al. 1996) from the National Centers for Environmental Prediction/National Center for Atmospheric Research (NCEP/NCAR) are used for the years 1979-2004. Analyzed fields include heights, winds, and streamfunction at 850 hPa and 200 hPa. The daily grid-point values were averaged over the 25 years to determine the climatological mean annual cycle. To construct the daily anomalies for each field, the mean for each grid point for each day was subtracted from the daily data. This method was chosen to minimize the influence of the annual cycle (Madden 1976). The second set of data used for this study is the 2.5° latitude by 2.5° longitude global, gridded National Oceanographic and Atmospheric Administration (NOAA) Interpolated Outgoing Longwave Radiation (OLR) (Liebmann and Smith. 1996) for the period 1979-2001. In this study, OLR data are used as a proxy for deep convection between 30°S and 30°N.

## B. EMPIRICAL ORTHOGONAL FUNCTION ANALYSIS

Empirical orthogonal function (EOF) analysis (Lorenz 1956) was used to identify the circulation patterns associated with the 700-hPa height anomaly field in the SH. The use of the EOF technique allowed for the identification of standing oscillations as well as the identification of transitory features. Distinct advantages of this type of analysis are that it extracts the patterns in the data that explain the maximum amount of variance as well as allowing for multivariate analysis of meteorological fields in both time and space.

For this study, an S-mode EOF analysis (Richman 1986) was performed to define the principal structures of variability in the spatial domain. Principal components (PC) define the variability in the time domain. The PCs can then be subjected to a time series analysis

## C. WAVELET ANALYSIS

Wavelet analysis allows the transformation of data from a one-dimensional time series to the dimensions of time and frequency. Wavelet analysis is ideal for datasets that exhibit non-stationarity in their statistics (Torrence and Compo 1998) as it identifies the distribution of variance at each time point. Analogous to Fourier spectra, a global wavelet spectrum can be calculated by averaging the amplitudes over time. Averaging over all times provides an unbiased and consistent estimate of the true power spectrum by giving more estimates at each point, as well as increasing the degrees of freedom at each point (Torrence and Compo 1998).

The specific mother wavelet chosen for this work was the Morlet wavelet, with the nondimensional frequency set to six. The wavelet analysis technique was applied to the PCs of the SH 700-hPa height anomaly fields to determine the dominant timescales of variability for the SH flow regimes. Wavelet analysis was also applied to the indices created from the tropical Atlantic variables. The application of wavelet analysis techniques allowed for a more meaningful comparison of the signals.

## D. LINEAR REGRESSION

Ordinary least squares linear regression (Wilks 1995) is a simple, yet effective and efficient method of determining the linear relationship between a predictor and a predictand. A distinct advantage of linear regression is that the method is completely objective in defining the relationship between the base index and the global field.

For this study the tropical North Atlantic was defined as the area from 10°W - 60°W and from the equator to 20°N, which is consistent with DeMaria (1999). An index based on 850-hPa zonal wind anomaly in the area 0-10°N, 20°W-60°W was used to as a measure of changes in the background low-level relative vorticity over the tropical North Atlantic. An index based on OLR anomalies (OLRA) in the area 5°N-15°N, 10°W-10°E, was used to define convection associated with the WAM. These indices were used as predictands in separate regression analyses.

The process for conducting the linear regression on the 850-hPa zonal wind anomaly in the tropical Atlantic is presented here. For the time period from 1 June – 31 October, for 23 years, 1979-2001, the 10-30-day filtered streamfunction anomalies at 200 hPa and 850 hPa, for the global grid, were regressed against a 10-30-day filtered version of the zonal wind anomaly index defined above. Furthermore, the regressions were evaluated by lagging the streamfunction fields from 15 days prior and 15 days after the zonal wind index. By using the method of ordinary least squares (Wilks 1995), the following equation was solved for a and b at each gridpoint for each lag,

$$\Psi_{i,j} = a_{i,j,lag} + b_{i,j,lag} U'$$

In this equation, $\Psi$ is the anomalous streamfunction, a is the ordinate intercept of the best fit line that represents the linear relationship between *U'* and $\Psi$, b is the slope of the best fit line that represents the linear relationship between *U'* and $\Psi$, $U'$ represents the anomalous zonal wind and *i* and *j* are the indices of corresponding the grid points on which the calculations were performed. The subscript *lag* is used to explicitly show that a and b are not equal for each lag.

Using the values for a and b calculated from the above equation, the following equation was used to predict the anomalous streamfunction at each point on the grid, *i* and *j*, that correspond to a zonal wind index of the mean plus one standard deviation, $u'_{significant}$.

$$\hat{\Psi}_{i,j,lag} = a_{i,j,lag} + b_{i,j,lag} u'_{significant}$$

The difference between $\Psi$ and $\hat{\Psi}$ is that $\Psi$ is the anomalous streamfunction value from the time filtered data but $\hat{\Psi}$ is the predicted value of the anomalous streamfunction based on the linear portion of the relationship between $\Psi$ and *U'*.

A similar procedure was followed using time filtered, anomalous OLR over Western African as the predictand in the regression. In addition to time-filtered streamfunction anomalies, time-filtered OLR anomalies and horizontal winds (the *u* and *v* components) were processed as predictors in the regression.

The statistical significance of the correlation between streamfunction and zonal wind anomaly at each point was assessed using a two-tailed student's *t*-test. A correlation coefficient of 0.27 is locally significant at the 5% level, based on 50 degrees of freedom.

## E. E-VECTOR ANALYSIS

Examination of transient circulations with respect to the influence on the time-mean flow can accomplished via the **E**-vector (Hoskins et al. 1983). The **E**-vector provides a representative indication of the group velocity of the transient circulations. Hoskins et al. (1983) defined a two dimensional quasi-vector **E**, such that,

$$\mathbf{E} = (\overline{v'^2 - u'^2}, \overline{-u'v'})$$

in which $u$ and $v$ represent the zonal and meridional components of the wind, respectively. Apostrophe notation indicates a deviation from the time-mean, while the overbar $(\bar{})$ represents a time average.

Kiladis (1998) applied this vector to a lagged cross-correlation analysis to further illustrate the nature of the wave activity in the North Pacific as related to the forcing of convection in the East Pacific Intertropical Convergence Zone. The advantage of using **E**-vector analysis is that the quasi-vector can characterize both the mean anisotropy, $\overline{v'^2 - u'^2}$, and the northward flux of westerly momentum, $\overline{u'v'}$. In this study, the **E**-vector is used as a diagnostic tool and is employed similarly to the study of Kiladis (1998).

## F. CASE STUDY

Composite charts were constructed for specific occurrences of SH midlatitude impacts on tropical Atlantic circulations. To determine the time periods to include in the composites, specific cases were chosen by visual inspection of plots of the zonal wind anomaly and OLRA indices. The days chosen to include in the composite charts were those associated with critical values of the two indices. For each day chosen, charts of time filtered streamfunction, total winds, and OLRA were generated. Circulations in the

regions of the world identified as having a significant relationship with the tropical Atlantic by the regression analysis were identified and tracked to determine their progression in time, as well as their relevant contribution to the anomaly in the base region.

THIS PAGE INTENTIONALLY LEFT BLANK

# III. ANALYSIS

## A. LARGE-SCALE SOUTHERN HEMISPHERE VARIABILITY

Large-scale structure and variability of the SH atmosphere are identified by performing an EOF analysis on daily 700-hPa height anomalies for 1979-2004. The NCEP/NCAR reanalysis fields are interpolated to a coarser resolution grid with five degree latitudinal spacing for the region from 20°S -90°S and 10 degree longitudinal spacing around the globe. The resulting data array, $X_{M,N}$, where M represents the spatial domain of 540 grid points (15 points in lat. X 36 points in lon.) and N represents the time domain of 9125 daily time steps (25 years with leap days removed). A covariance matrix, $C= XX^T = C_{M,M}$ , was calculated to determine the degree to which each daily 700-hPa height anomaly is related to every other. The EOF analysis of the covariance matrix results in eigenvectors that define the orientation at which the data jointly exhibit a maximum amount of variation. Principal components (PC) are then computed by projecting the original anomaly field onto each eigenvector. The principal components then describe the time variation of each eigenvector as related to the original anomaly field. Finally, the original anomaly fields are projected on the normalized PCs.

By definition, the first EOF describes the greatest amount of variability and represents the predominant anomaly structures in the sampled data. Successive EOFs describe the structures that explain progressively smaller amounts of variance. The leading mode is commonly associated with the AAO (Burton 2005), and is not discussed further in this study. Modes 2 and 3 collectively explain approximately 11 percent of the total variance in the original data set.

As discussed in Chapter I, section B, EOF 2 and 3 represent a propagating wave train from the South Pacific into the South Atlantic. While the study by Burton (2005) concentrated on the relationship of EOF mode 1 to tropical convection in the Indian Ocean and Western Pacific monsoon trough, there was little mention of higher modes. However, the focus of the current study

is on transient SH circulations, which are represented by modes 2 and 3. The PC associated with EOF 2, was analyzed to determine the seasonal nature of the PC for the years 1979-2004. Monthly variances of the daily PC 2 index (Figure 3.1) indicate that the maximum variability in EOF 2 occurs during the boreal summer.

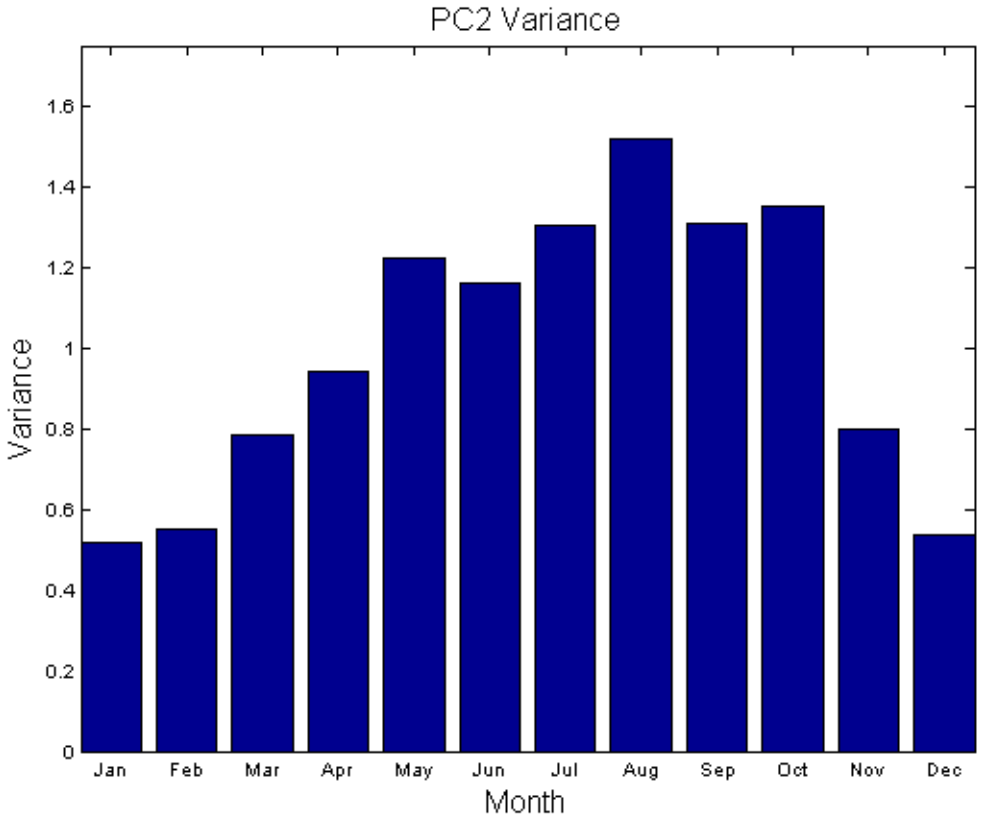


Figure 3.1 Monthly variance (unitless) of principal component 2 of the 700-hPa height anomaly EOF analysis from 1979-2003

The global wavelet spectrum (Figure 3.2) of PC 2 indicates that the series contains statistically significant variance on many time scales, including decadal, interannual and intraseasonal. These results are consistent with the discussion provided by Mo and Paegle (2000) in that PC 2 was found to have significant variance on a range of time scales, including the quasi-biennial and intraseasonal time scales.

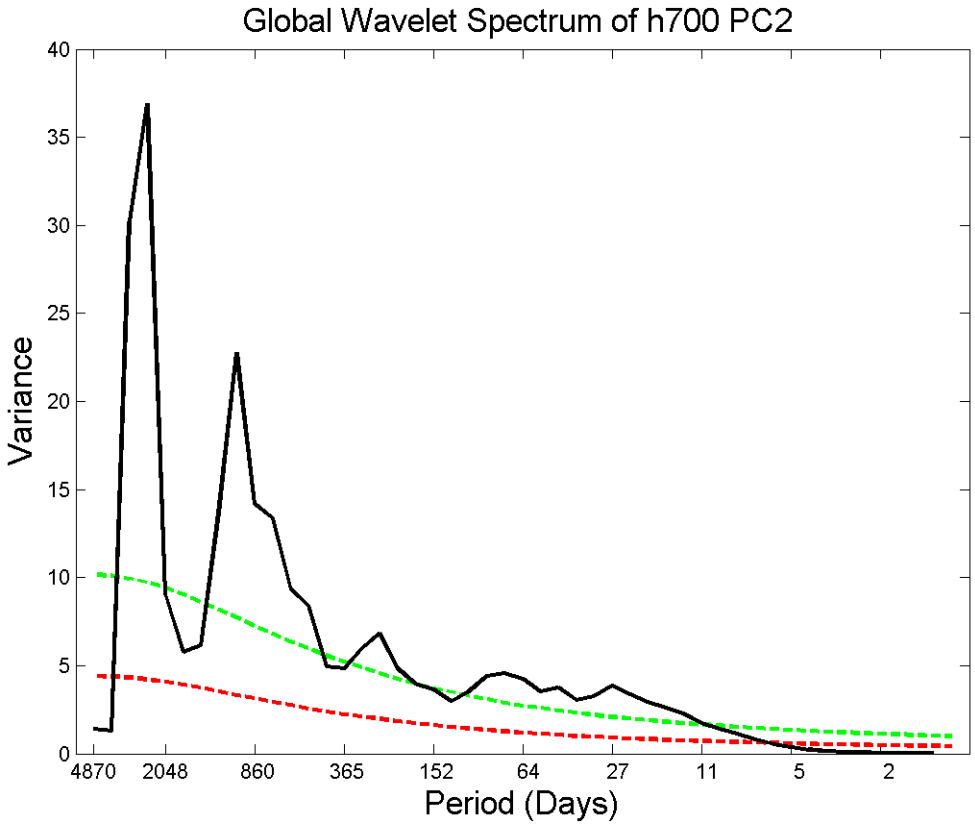


Figure 3.2 Global wavelet spectrum (solid line) of the daily values of PC2 of the 700-hPa height anomaly EOF analysis from 1979-2003. Upper dashed line (green) is the 99% confidence spectrum and the lower dashed (red) line is a red noise spectrum based on a univariate lag-1 autoregressive process.

Based on the significant amount of variance in the 10-30 day period (Figure 3.2), the original 700-hPa height anomaly data were filtered using a Lanczos filter (Duchon 1979) for this range. The filtered data were then subject to the same EOF procedure detailed above.

The filtered EOF 2 (Figure 3.3), which explains 8.9% of the variance in the filtered data, defines a wave train similar to that present in the unfiltered EOF 2 (Figure 1.2). Also, there is evidence of equatorward propagation of wave activity from the SH midlatitudes over the South Pacific. However, one difference between the filtered EOF 2 and the unfiltered EOF 2 is that the filtered EOF 2 exhibits larger variability over the Indian Ocean.

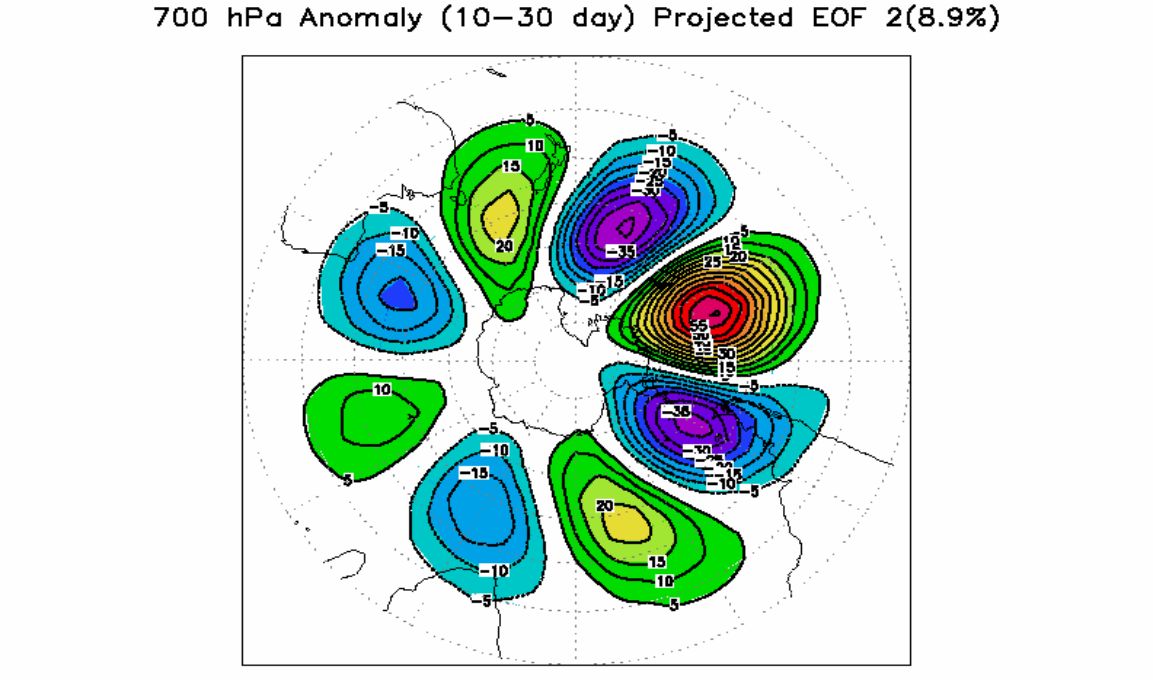


Figure 3.3 700-hPa height anomalies (m) from 1979-2003 regressed onto the second EOF pattern of 10- to 30-day filtered 700-hPa heights. Contour interval is 5 m. Negative contours are dashed.

The filtered EOF 3 (Figure 3.4), which explains 8.1% of the variance in the filtered data set, is similar to EOF 3 of the unfiltered data. As in Burton (2005), EOF 3 is in near quadrature with EOF 2, and both show a significant wave train with maximum amplitude in the South Pacific. A key feature evident in the filtered EOF 3 is equatorward propagation of wave activity in the South Atlantic that is directed toward Africa. Both EOF 2 and EOF 3 of the filtered data are similar to what was shown in Kiladis and Mo (1998).

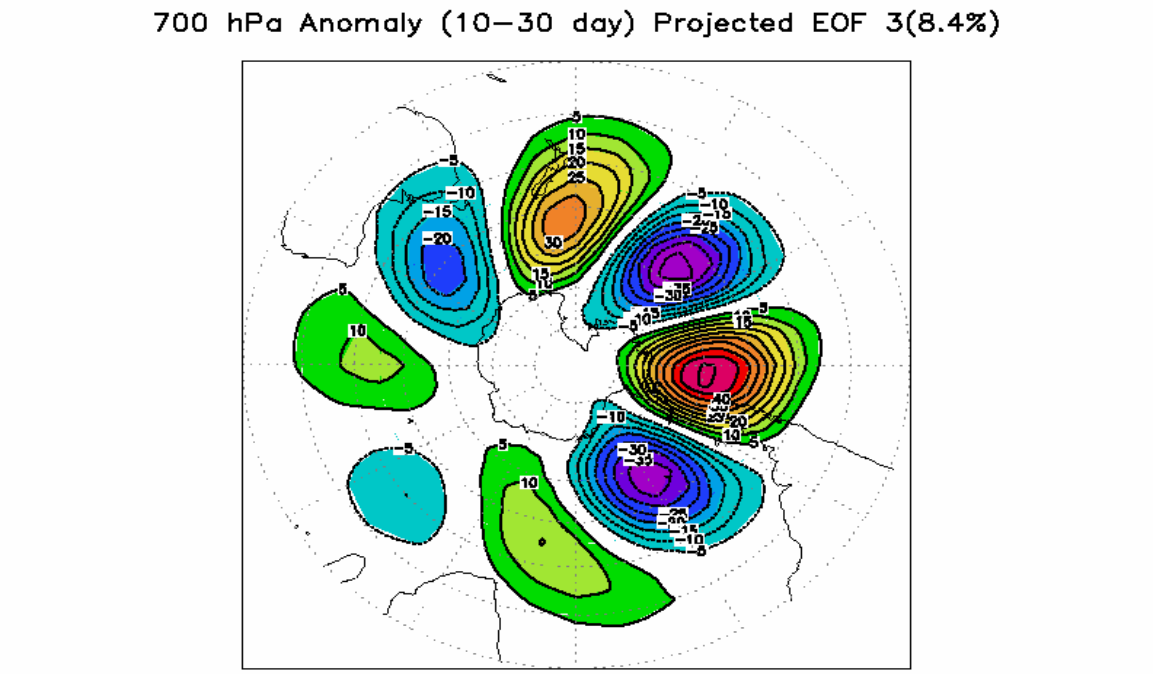


Figure 3.4 As in Figure 3.3 except for the third EOF of the filtered 700-hPa heights.

## B. CHARACTERISTICS OF THE ZONAL WIND AND CONVECTION INDICES

To determine the dominant oscillation periods in the index of the zonal wind and the index of convection over the region of the WAM, wavelet analysis was also applied to each time series. In comparison with the global wavelet spectrum of PC 2, the global wavelet spectrum of 850-hPa zonal wind index (Figure 3.5) also contains significant variance in the 10-30-day range. Therefore the winds and streamfunction fields are also bandpass filtered around the 10-30 day period. Sultan et al (2003) presented the results of a wavelet analysis of a daily rainfall index for West Africa, which exhibited significant variance on the same intraseasonal time scale.

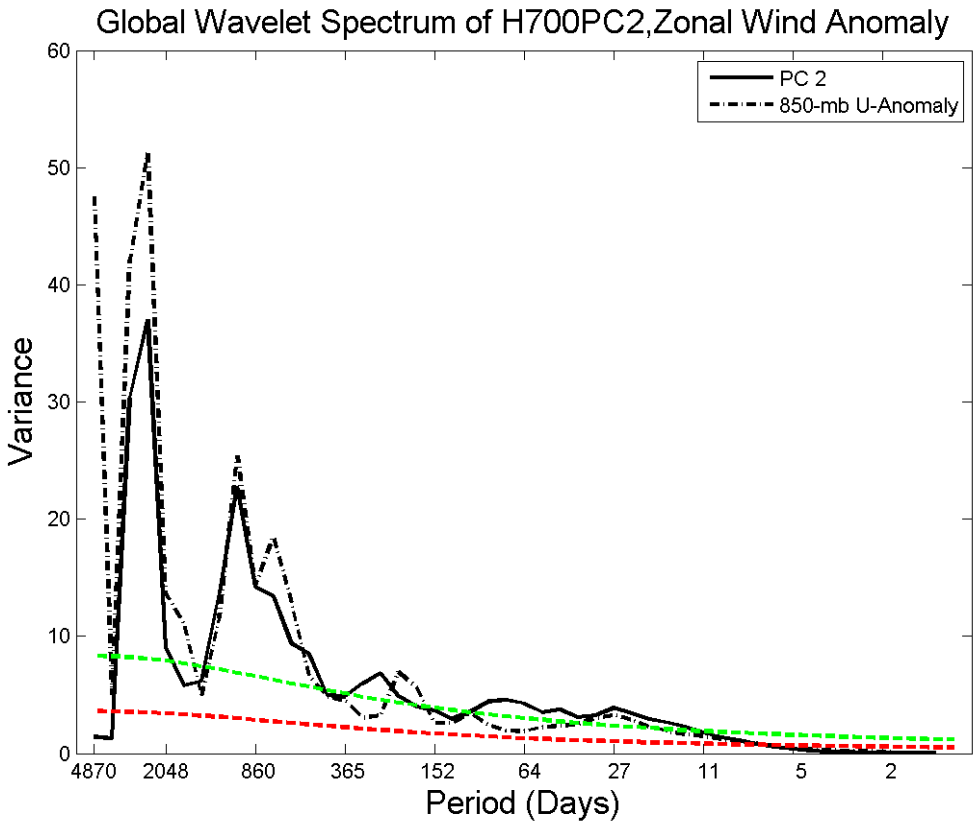


Figure 3.5 As in Figure 3.2, but for the global wavelet spectrum of the 850-hPa zonal wind anomaly in the tropical Atlantic is added.

## C. REGRESSION ANALYSIS

### 1. Background

Increased low-level vorticity across the tropical North Atlantic will contribute to an environment that will be favorable for the growth of easterly waves that begin over Africa. In this study, a westerly zonal wind anomaly in the southern half of the tropical Atlantic is used to represent an increase in the relative vorticity of the region. Therefore, the global-scale circulation anomalies associated with a significantly positive value of the 850-hPa zonal wind index are defined by regressing the 850-hPa and 200-hPa streamfunction and horizontal winds (both the zonal and meridional components) on the zonal wind index. Also, OLR is regressed on the zonal wind index. The index of West African OLRA is also used as a base variable on which streamfunction, total winds, and OLRA are regressed to define global-scale circulations associated with variations in convection during the WAM.

### 2. 200-hPa / 850-hPa Streamfunction Regressions on Zonal Wind

As defined above, the regression patterns are scaled to a significantly positive zonal-wind index value. Upon inspection of the regression patterns over lags of -15 to +15 days, it became evident that a relative minimum in the zonal wind index occurred near lags of -8 and +8 days. Therefore, the lagged regression maps in the interval -8 to +8 days, are examined in this section.

#### *a. Lag -8 Days*

At lag -8 days, it is clear that easterly wind anomalies exist at low-levels across the equatorial Atlantic (Figure 3.6b). At 200 hPa (Figure 3.6a), there is a SH wave train that extends from the anticyclonic anomaly in the equatorial central Pacific, toward South America then curves equatorward over the Southern Atlantic. Over the equatorial central Pacific, the anticyclonic couplet that straddles the equator near 160°W suggests that the SH wave train may be related to an equatorial Rossby wave and convective patterns associated with the equatorial wave. At 850 hPa (Figure 3.6b), the SH wave train between 160°W and 0°W is also a dominant feature of the regression map. The anticyclonic anomaly at approximately 10°S, 30°W is associated with the easterly anomalies across the equatorial Atlantic. Furthermore, the presence of a low-level anticyclone in the equatorial South Atlantic in association with an increase in rainfall during the WAM is consistent with the findings of Sultan et al. (2003). This is reflected by the negative OLRA over the Gulf of Guinea region of Western Africa. Another significant feature present is strong southerly flow on the western side of a cyclonic anomaly near 40°S and 40°W. This suggests the beginnings of a deep cold surge from the south called a *friagem*, which is a common occurrence in the austral winter (Satyamurty et al. 1998). Finally, there is an indication in the 850-hPa anomalous circulations that the central Pacific circulations may be a source region for the SH midlatitude wave train.

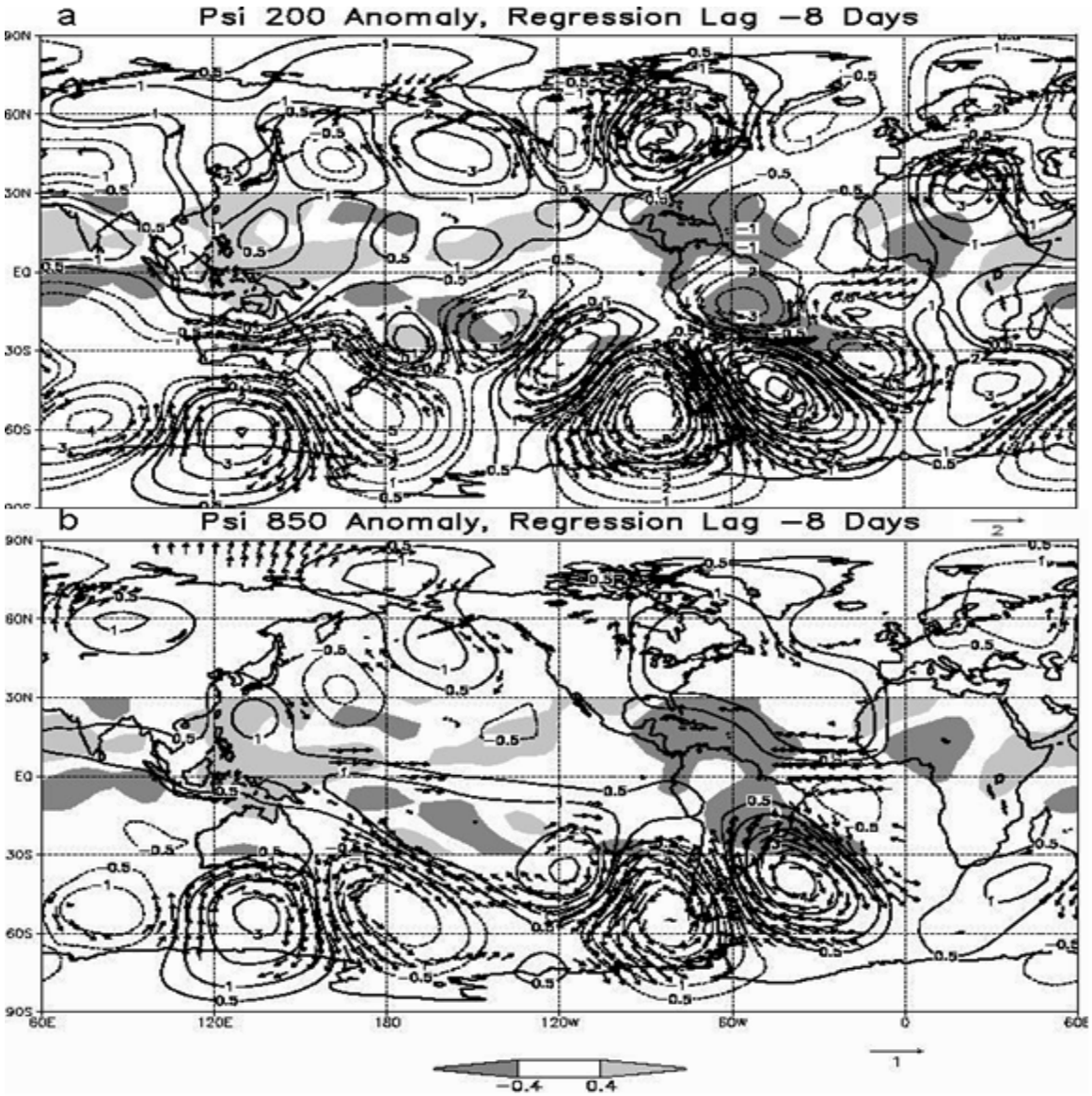


Figure 3.6 (a) Streamfunction anomaly at 200 hPa ($10^6$ $m^2$ $s^{-1}$) and OLR (W $m^{-2}$) anomalies in the 10-30-day band during June-Oct 1979-2001 associated with a zonal wind anomaly of +1 standard deviation in the base region 0-10°N, 60°W-10°W. Wind vectors are plotted where the local correlation coefficient is significant at the 95% confidence limit. OLR anomalies are shaded according to the color bar. Reference wind vector is in the bottom right corner. (b) As in (a), except for 850-hPa.

### *b. Lag -6 Days*

At lag -6 days, the primary 200-hPa circulation anomalies (Figure 3.7a) in the SH wave train have propagated eastward. There is an indication that the cyclonic anomaly near 40°S, 120°W and the cyclonic anomaly near 70°S, 120°W began to merge. Also, the OLRA associated with convection in the WAM has expanded in areal extent.

There is little change in the 850-hPa structure from lag -8 days to lag -6 days (Figure 3.7b). The negative OLRA over Brazil has developed on the eastern side of the cyclonic anomaly, which is consistent with results in Liebmann et al. (1999). The OLRA over western Africa has expanded in association with the anticyclonic anomaly over the South Atlantic near 15°S, 10°W. Although the winds in the eastern portion of the South Atlantic anticyclonic anomaly are not statistically significant, the increase in convection over Western Africa corresponds to the southerly flow over the Gulf of Guinea as defined by Grodsky and Carton (2001) and Sultan et al. (2003).

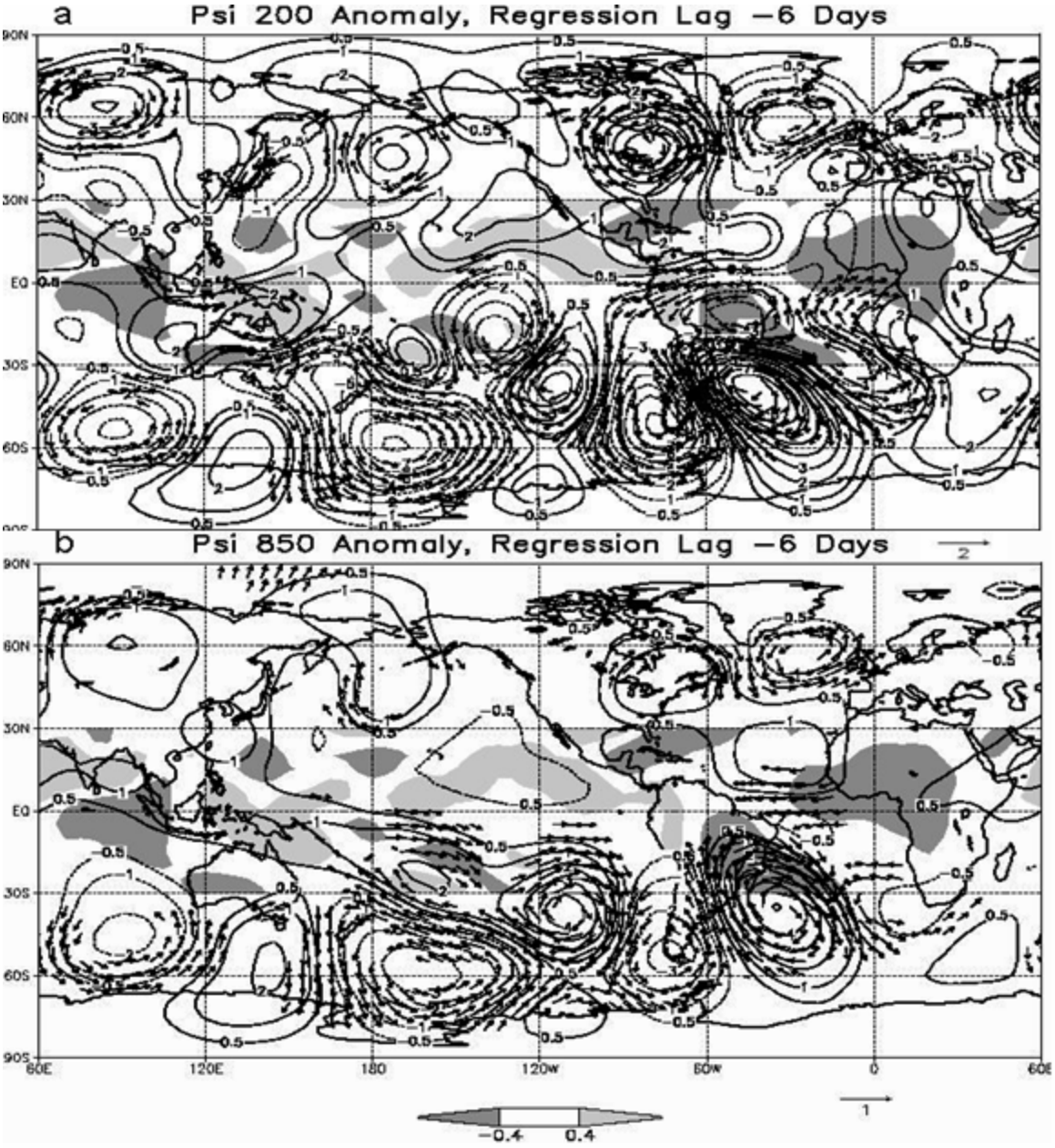


Figure 3.7 As in Figure 3.6, except for lag -6 days.

### *c. Lag -4 Days*

At upper levels (Figure 3.8a), the cyclonic circulations along 110°W have continued to merge. All circulations contained in the SH wave train over South America have become oriented northwest to southeast, which implies equatorward eddy propagation over the southern half of South America (Hoskins et al, 1983). In the tropical Atlantic, the cyclonic circulation near Sub-Saharan Africa has weakened and moved off to the southeast, which results in a lull in the 200-hPa winds in the eastern half of the tropical Atlantic. Concurrently, an anticyclone has moved from the Amazon Basin into the equatorial South Atlantic, which caused an increase in the 200-hPa westerlies over the northern portions of South America. The area of negative OLRA over equatorial eastern Atlantic and Western Africa has increased from lag -6 days.

At 850-hPa (Figure 3.8b) all circulations in the primary SH wave train have moved eastward. The ongoing merger of the cyclonic anomalies along 110°W has resulted in a large cyclonic anomaly west of Chile. The cyclonic anomaly southeast of Brazil has shifted equatorward. The anticyclonic anomaly over the equatorial South Atlantic at lags -8 and -6 days has dissipated. Therefore, the zonal wind anomalies over the equatorial Atlantic are no longer significant.

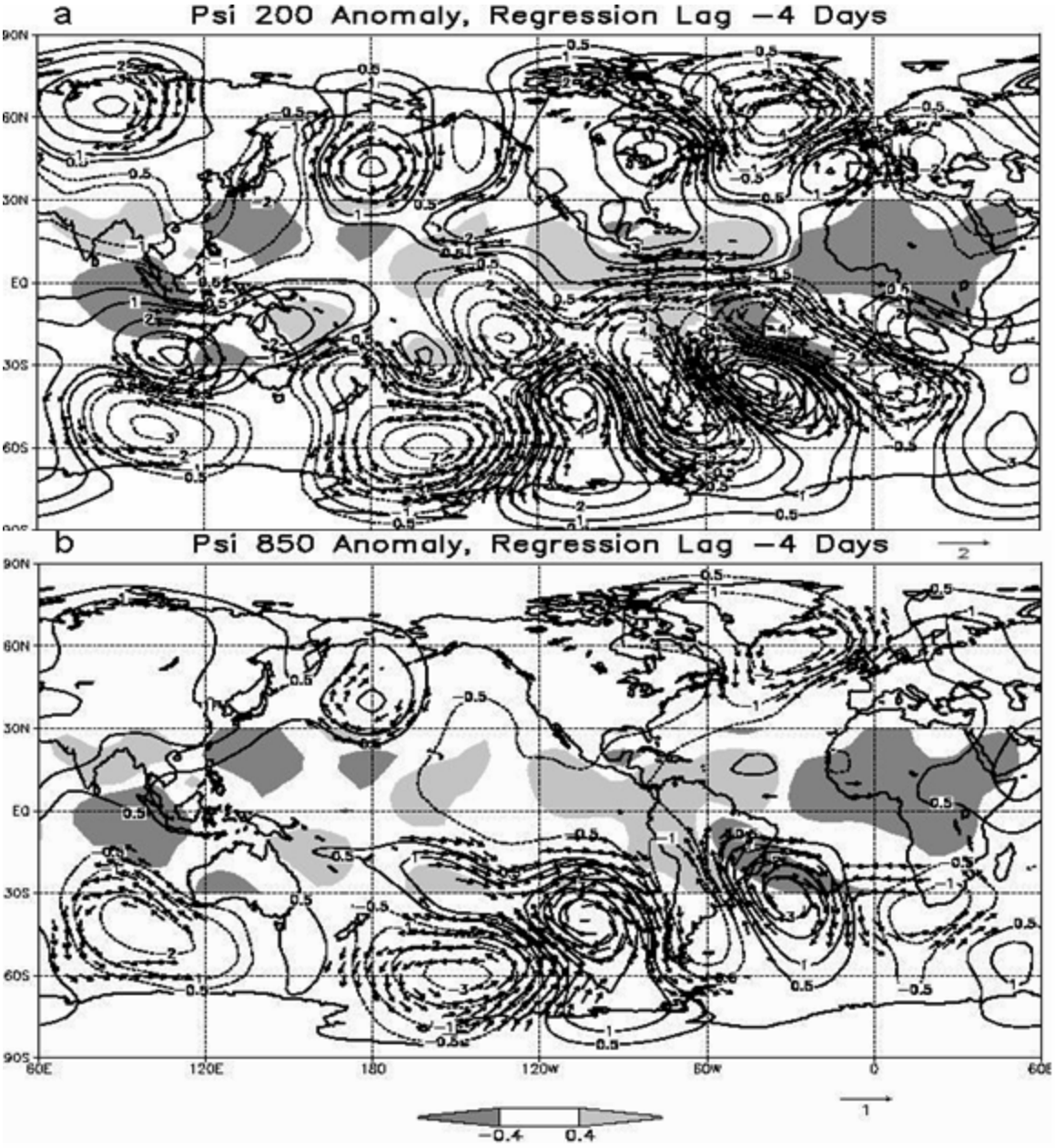


Figure 3.8 As in Figure 3.6, except for lag -4 days.

### *d. Lag -2 Days*

At 200-hPa (Figure 3.9a), the merger of the cyclonic anomalies over the southeastern Pacific has resulted in a large cyclonic anomaly off the west coast of Chile. All circulations in the SH midlatitude wave train continue to become oriented from northwest to southeast, such that the anticyclonic anomaly over the South Atlantic has contributed to strong easterly winds over most of the equatorial Atlantic. The size of the negative OLRA associated with the WAM is no longer increasing.

The complete merger of the cyclonic anomalies in the southeastern Pacific is also evident at 850-hPa (Figure 3.9b), and the cyclonic anomaly west of Chile has increased in size. The anticyclonic and cyclonic anomalies over South America and the South Atlantic have shifted eastward and north respectively. The equatorward shift of the cyclonic anomaly over the South Atlantic has resulted in westerly anomalies over the equatorial Atlantic. This result is consistent with the results of Sultan et al. (2003) in that a low-level cyclonic circulation on the southern side of the equator in the Atlantic was associated with a peak and the subsequent reduction in convection over West Africa. Furthermore, the baroclinic structure of the near-equatorial anomalies has resulted in low-level westerly anomalies and upper-level easterly anomalies over the equatorial Atlantic.

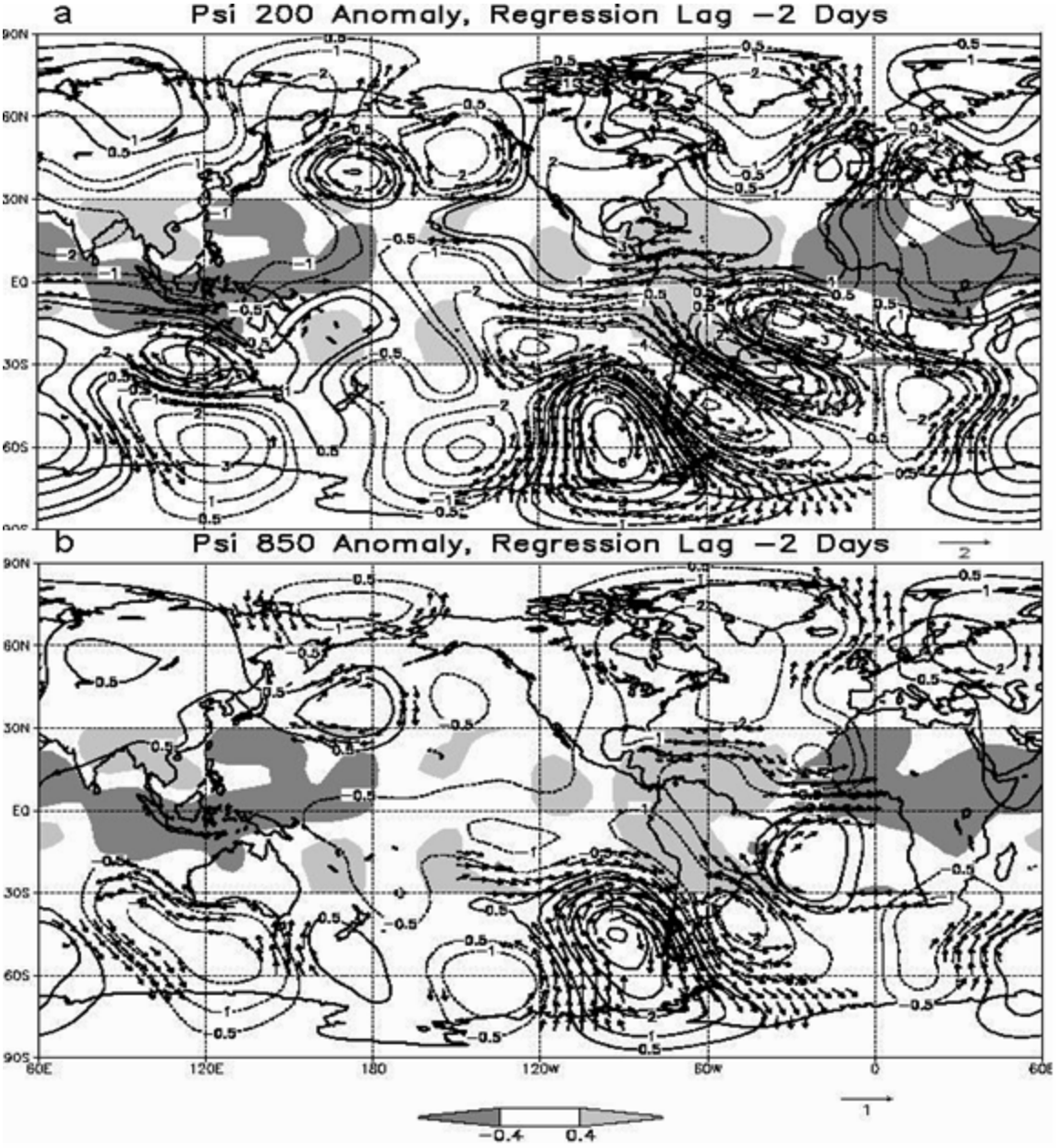


Figure 3.9 As in Figure 3.6, except for lag -2 days.

### *e. Lag 0*

The simultaneous regression at 200-hPa (Figure 3.10a) defines a wave train that makes a sharp arc from the equatorial central Pacific, toward the SH midlatitudes, and then into the tropical Atlantic. This wave train is nearly 180° out of phase with the wave train present at lag -8 days. Also, the convective signal in the WAM has reversed sign from lag -8 to lag 0, with the region of negative OLRA moving west, out over the tropical Atlantic and an area of positive OLRA centered over Nigeria.

The simultaneous regression chart for 850 hPa (Figure 3.10b) contains a wave train that is strongly related to the SH midlatitudes and extends toward the tropical Atlantic. The cyclonic anomaly over the South Atlantic has strengthened, as have the westerly wind anomalies in the tropical Atlantic. Also, the anticyclonic anomaly southeast of Brazil has intensified with strong southerly wind anomalies, indicating a relation with the cold surge event (*friagem*) (Satyamurty et al. 1998). There is a first baroclinic mode structure in the tropical Atlantic, but an equivalent barotropic structure present in the midlatitudes.

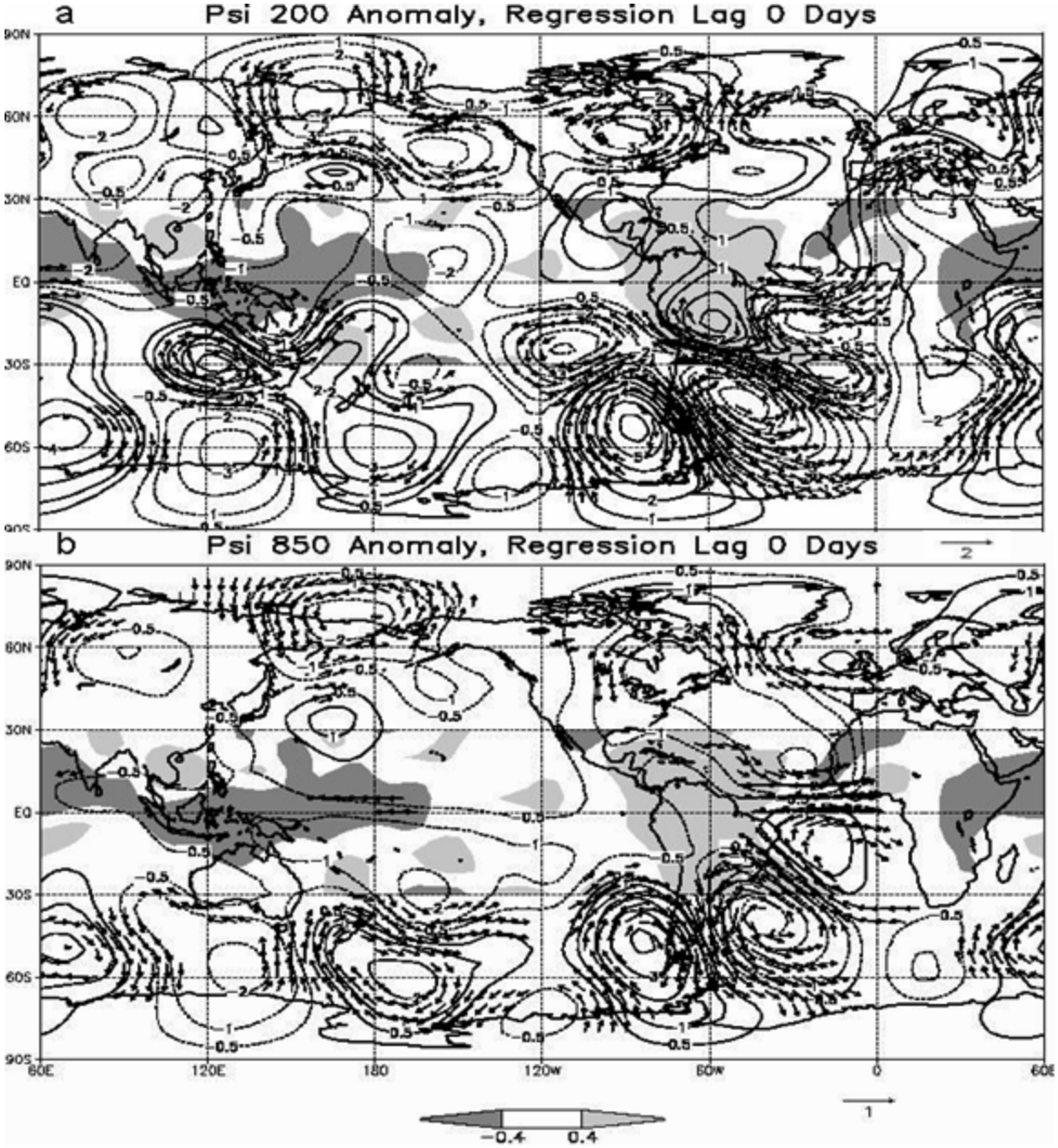


Figure 3.10 As in Figure 3.6, except for a simultaneous regression.

### *f. Lag +2 Days*

At upper-levels, the SH wave train continues to be a predominant feature at lag +2 days (Figure 3.11a); however, all circulation anomalies have shifted eastward. The eastward motion of the upper-level anticyclonic anomaly over the South Atlantic has resulted in a corresponding eastward shift of the zonal wind anomalies over the equatorial Atlantic. The cyclonic anomaly over the Amazon Basin has strengthened and contributed to westerly wind anomalies along the equator over northern South America.

At 850 hPa (Figure 3.11b), the cyclonic anomaly west of Chile has dramatically decreased in intensity; however the downstream anticyclonic and cyclonic anomalies remain strong. In association with the cyclonic anomaly over the South Atlantic, the westerly wind anomalies over the equatorial Atlantic remain interestingly strong. The area of positive OLRA that was centered over Nigeria has expanded in coverage and now extends over the equatorial eastern Atlantic.

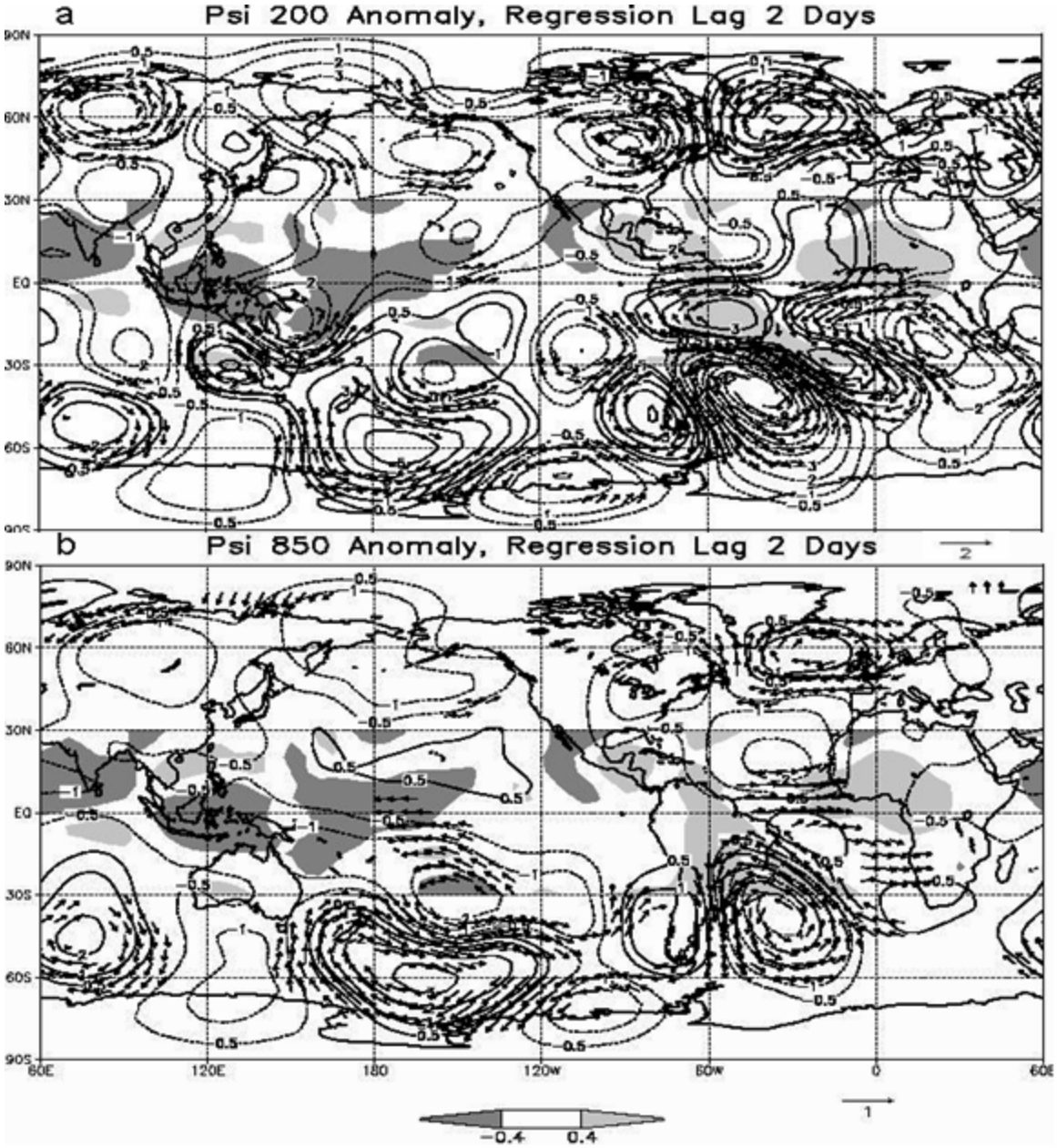


Figure 3.11 As in Figure 3.6, except for lag +2 days.

### *g. Lag +4 Days*

The wave train over South America and the South Atlantic continues to dominate the regression map at 200 hPa (Figure 3.12a). However, the circulations are becoming more zonally oriented and continue to shift eastward with less connection to the equatorial Atlantic. In association with the cyclonic circulation over the Amazon Basin, westerly wind anomalies have spread eastward, over the equatorial Atlantic.

At low-levels (Figure 3.12b), the circulation anomalies have weakened and become zonally oriented with no connection to the tropical Atlantic. There is evidence of the development of a large anticyclonic anomaly over the southeast Pacific. The area of positive OLRA over Africa has expanded.

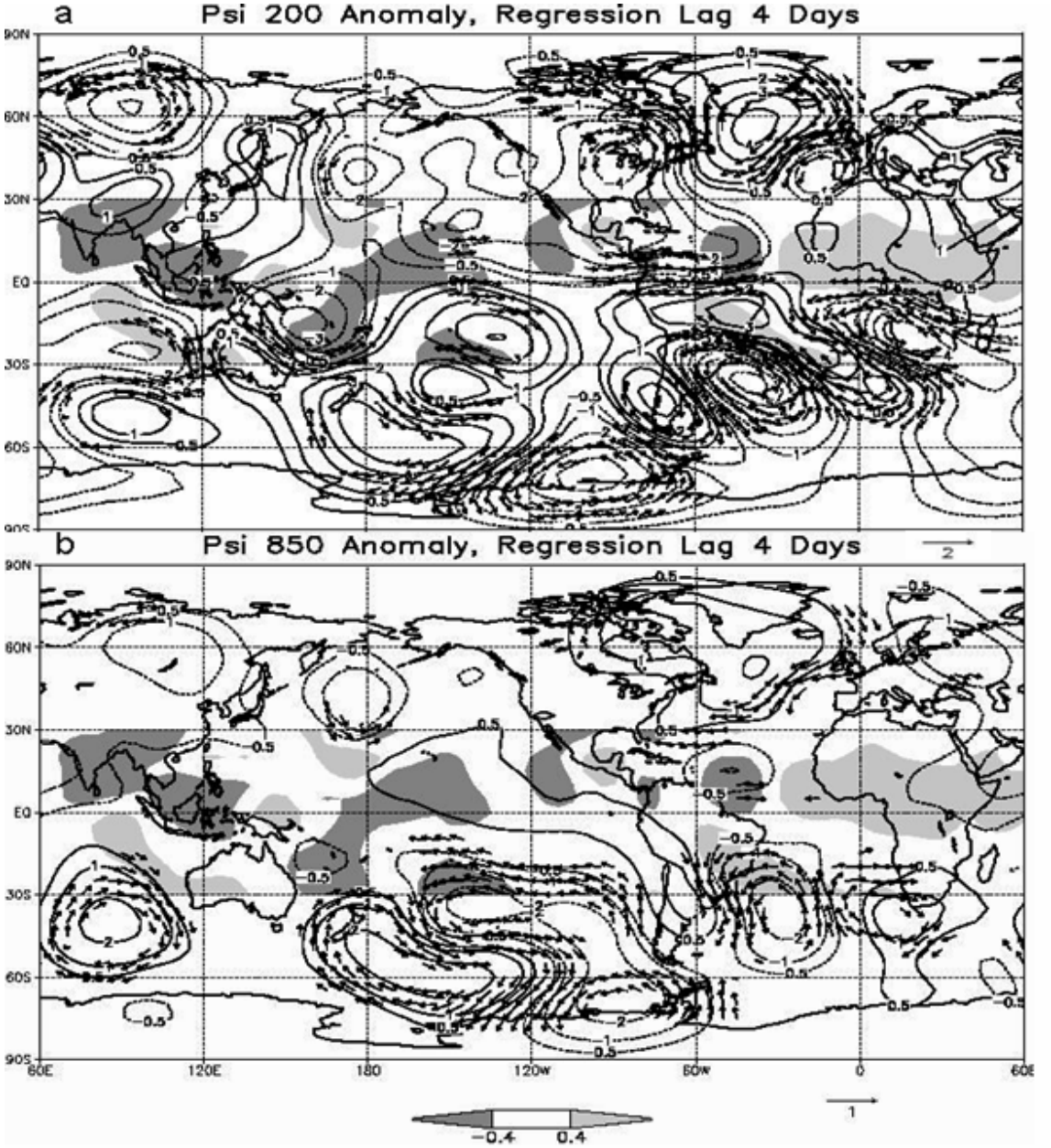


Figure 3.12 As in Figure 3.6, except for lag +4 days.

### *h. Lag +6 Days*

At upper-levels (Figure 3.13a), anomalous circulations over South America and the South Atlantic have evolved such that anticyclonic anomalies exist west of Chile. Alternating cyclonic and anticyclonic anomalies extend downstream of the anticyclonic anomaly west of Chile, toward the equatorial Atlantic.

At low-levels, there has been a corresponding shift in the circulation anomalies over South America and the South Atlantic. A large anticyclonic anomaly dominates the eastern South Pacific. A cyclone and an anticyclone extend northeastward, toward the equatorial Atlantic, such that easterly zonal wind anomalies now exist along the equator. This pattern, which features an anticyclone in the equatorial south Atlantic, will contribute to the start of onshore flow in from the Gulf on Guinea, which is similar to Figures 7 and 8 of Sultan et al. (2003), which defines circulation patterns seven days prior to and seven days after the onset of increased convection over western Africa.

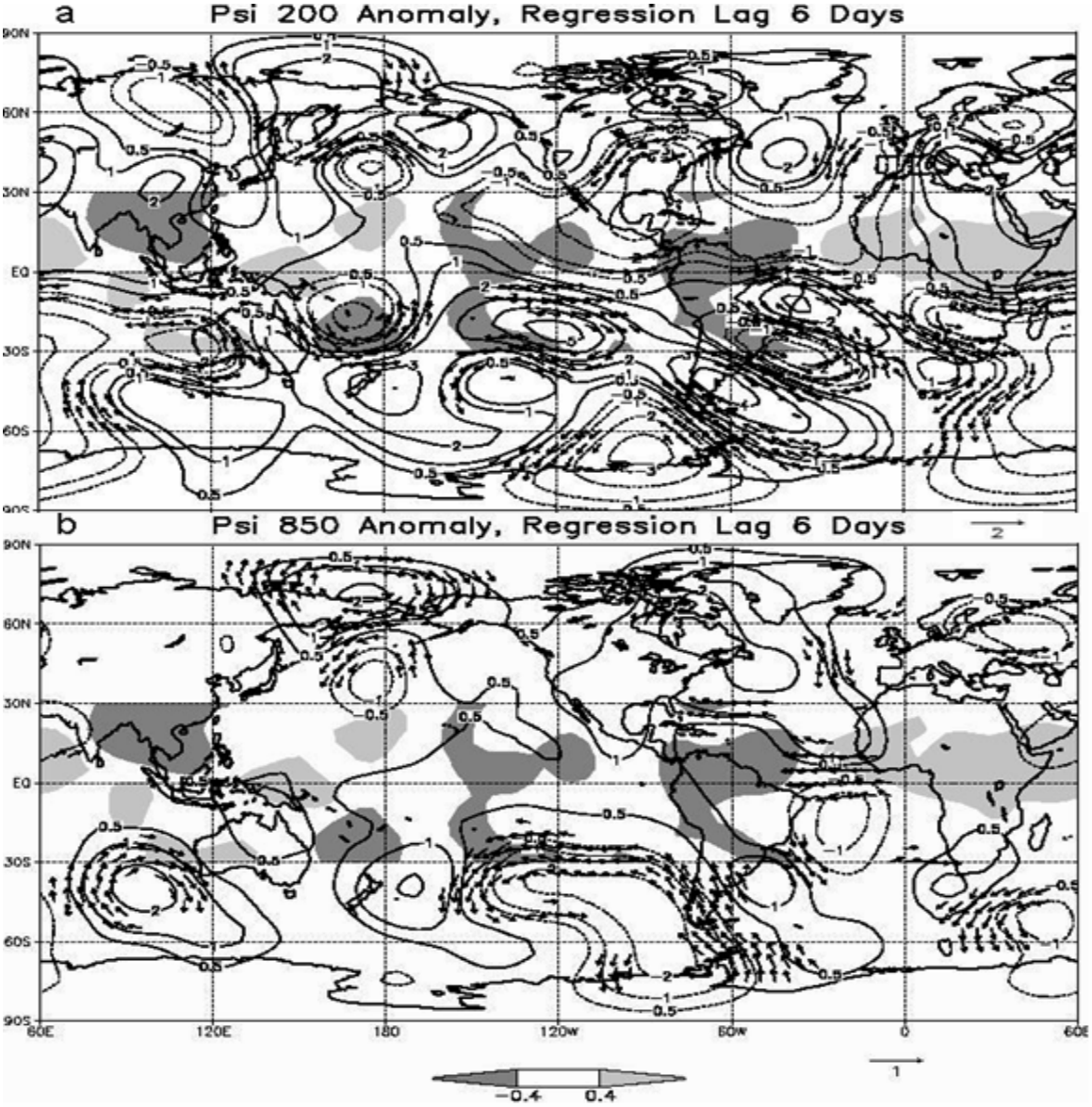


Figure 3.13 As in Figure 3.6, except for lag +6 days.

### *i. Lag +8 Days*

The 200-hPa circulations associated with the last stage in a full cycle of the base index (Figure 3.14a) indicate that convective activity associated with the WAM is beginning to change. The areal extent of positive OLRA over West Africa decreases. The circulation centers over the SH are somewhat disorganized.

At low-levels (Figure 3.14b), the SH circulation centers have weakened but still appear to constitute a pronounced wave train. The anticyclonic anomaly over the South Atlantic continues to contribute onshore flow over western Africa. This onshore flow was associated with the negative OLRA that was discussed in association with the negative lags as the cycle repeats itself.

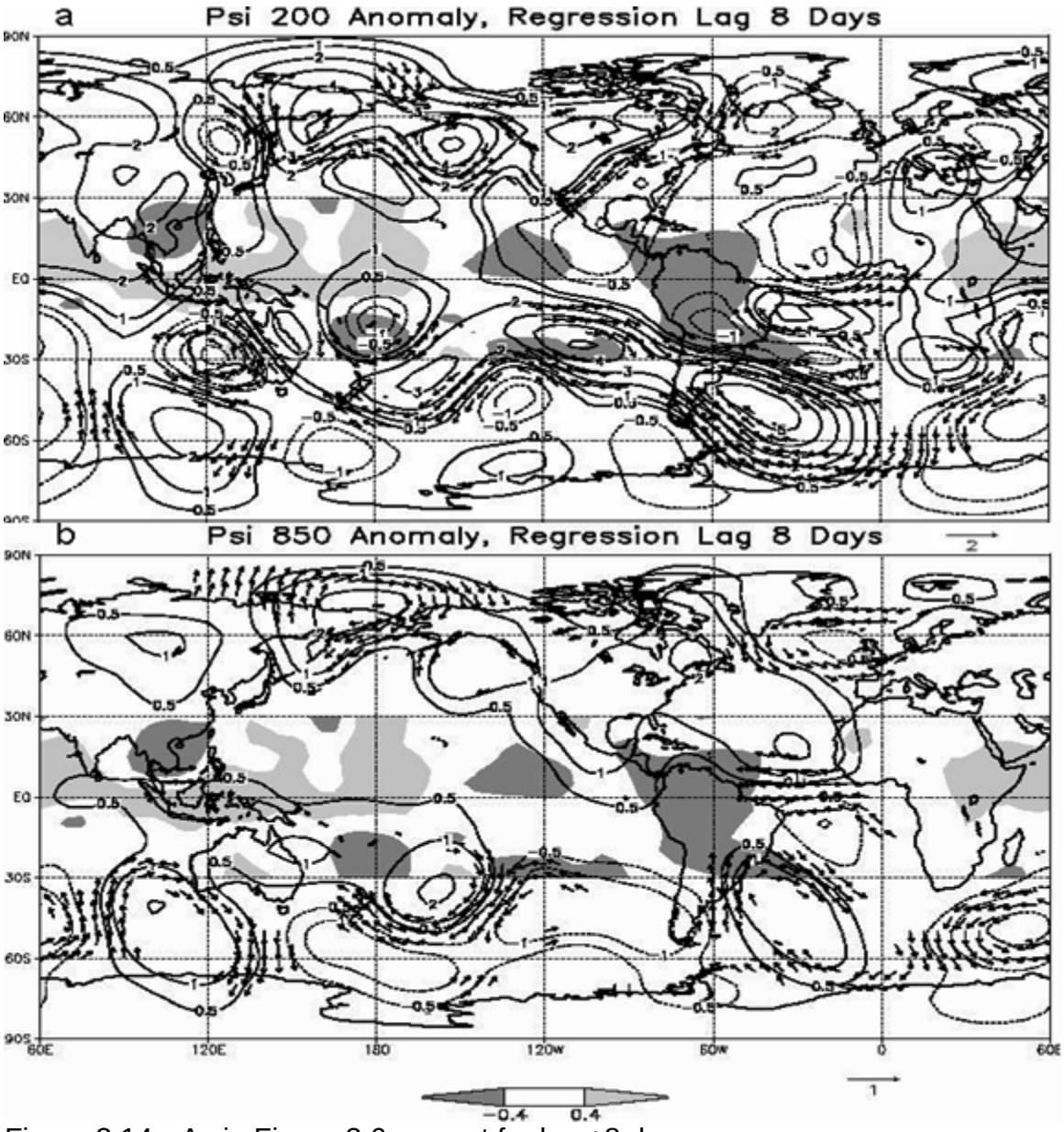


Figure 3.14 As in Figure 3.6, except for lag +8 days.

### *j. Summary*

The upper-level wave train that spans the southeast Pacific, South America and the South Atlantic may be initiated as a response to forcing over the equatorial central Pacific (Figure 3.6a). As a part of that wave train, between lags -8 days and -4 days (Figures 3.6-3.8) a strong cyclonic anomaly forms over the midlatitude, southeast Pacific and moves southeastward. Concurrently, a smaller high-latitude cyclonic anomaly propagates eastward and eventually merges over the southeast Pacific with the cyclonic anomaly contained in the original wave train. The completion of the merger between -4 days and -2 days results in a large cyclonic anomaly west of Chile. Although there are anomalous circulations over South America and the South Atlantic prior to lag-4 days, the presence of the strong cyclonic anomaly west of Chile at both 850 hPa and 200 hPa at lag -4 days coincides with an organization and intensification of the circulation anomalies over South American and the South Atlantic. The organization appears to be related to a cold surge into Southeastern Brazil and enhanced convection throughout the South Atlantic Convergence Zone. Furthermore, the evolution of the circulation anomalies that starts at lag -4 days lead to the movement of the low-level cyclonic anomaly toward the equatorial Atlantic and the initiation of westerly wind anomalies, that by definition reach their maximum at lag 0 (Figure 3.10).

Throughout the evolution of the circulation anomalies between lags -8 day and lag 0, there is a strong association between the wind anomalies over the equatorial Atlantic and OLRA over western Africa. It is clear that the negative OLRA occur after the formation of the subtropical anticyclonic anomaly over the South Atlantic, which is similar to the results of Sultan et al. (2003). By lag -2 days to lag 0, the region of negative OLRA moves over the equatorial Atlantic, with positive OLRA forming over western Africa in association with a cyclonic anomaly over the subtropical South Atlantic, which imposes flow from Africa toward the Gulf of Guinea. The relation between circulation and OLRA over western Africa is examined by a separate regression analysis, in which OLRA over western Africa are used as the base, i.e., the predictand.

### 3. 200-hPa / 850-hPa Streamfunction Regressions on OLR in the West African Monsoon

Based on the regression results from Section 2, it is clear that the westerly wind anomalies over the equatorial Atlantic follow the formation of the negative OLRA over western Africa. Therefore, the regression maps based on OLRA are only examined for lag 0 and positive lags.

#### *a. Lag 0*

By definition, at a lag of zero days there are significant negative OLRA over western Africa (Figure 3.15). Overall, the OLRA at lag zero define a global-scale pattern in which there are negative OLRA over the tropical western North Pacific and positive OLRA over the eastern North Pacific. At upper-levels (Figure 3.15a), there is some indication of a wave-train response emanating from the tropical western North Pacific. Furthermore, there may also be some response due to the lack of convection over the tropical eastern Pacific that may be contributing to the to the well-defined wave pattern over North and South America respectively. Similar but weaker features are evident at low-levels (Figure 3.15b).

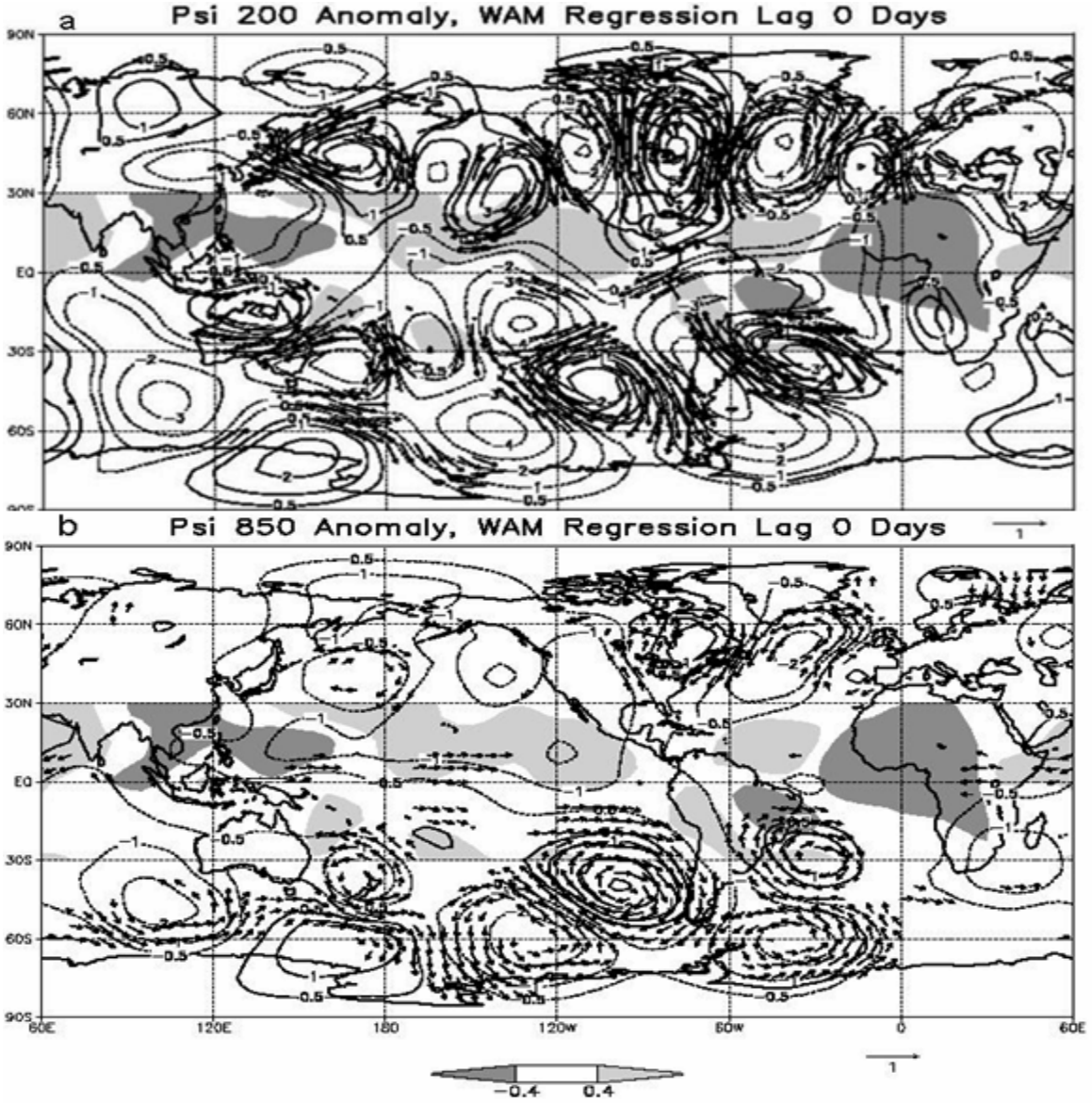


Figure 3.15 (a) 200-hPa regression map of streamfunction (contour interval, $10^6$ $m^2$ $s^{-1}$), winds (m $s^{-1}$), and OLR (W $m^{-2}$ ) anomalies in the 10-30 day band during June-Oct 1979-2001 associated with an OLR anomaly of +1 standard deviation in the base region 5-15°N, 10°W-10°E. Wind vectors plotted where local correlation coefficient is significant at the 95% confidence limit. OLR anomalies are shaded according to the color bar. Reference wind vector is in the bottom right corner.

### *b. Lag +2 Days*

At upper-levels (Figure 3.16a) a wave-like feature in both hemispheres is present. However, there appears to be more of an equatorward orientation over the SH midlatitudes between 120°W and 0°W. This is similar to the preferred wave path defined by Ambrizzi et al. (1995).

At low-levels (Figure 3.16b), the wave pattern over the SH is less evident. However, westerly zonal wind anomalies do begin to appear over the equatorial South Atlantic. The westerly zonal wind anomalies are related to twin cyclonic anomalies that straddle the equator near 25°W, which is again similar to Sultan et al. (2003).

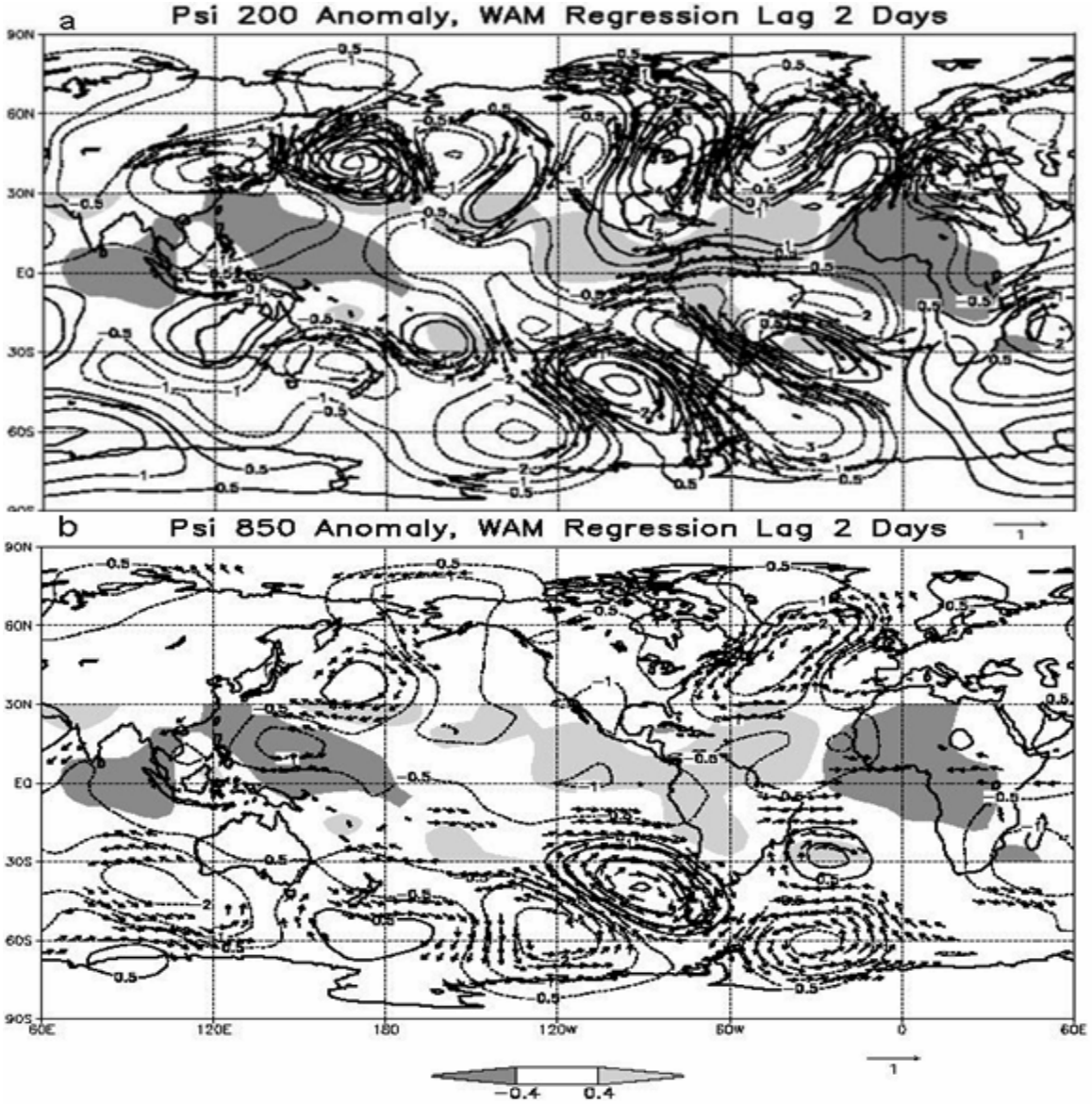


Figure 3.16 As in Figure 3.15, except for lag +2 days.

### *c. Lag +4 Days*

At upper-levels (Figure 3.17a), the circulations in the SH wave train between 120°W and 0°W move east and equatorward. The negative OLRA over western Africa extend toward the equatorial Atlantic. The strong upper-level anticyclonic circulation that straddles the equator along 30°W contributes to upper-level easterly anomalies along the equator and west of the region of negative OLRA over western Africa.

At lower levels, (Figure 3.17b), westerly anomalous winds are found throughout the equatorial Atlantic. Therefore, there is a baroclinic structure to the equatorial anomalies such that westerly anomalies occur at low-levels ahead of enhanced convection and easterly anomalies are found at upper-levels ahead of the enhanced convection. Furthermore, there seems to be no significant correlation between midlatitude circulation anomalies and the zonal wind anomalies over the equatorial Atlantic, as was found in the regression based on the zonal wind index.

The lagged regression maps imply a 4-day time lag between the time of maximum convection in the WAM and the time of maximum low-level zonal wind anomalies in the tropical Atlantic. This 4-day time lag is consistent with the results of Sultan et al. (2003).

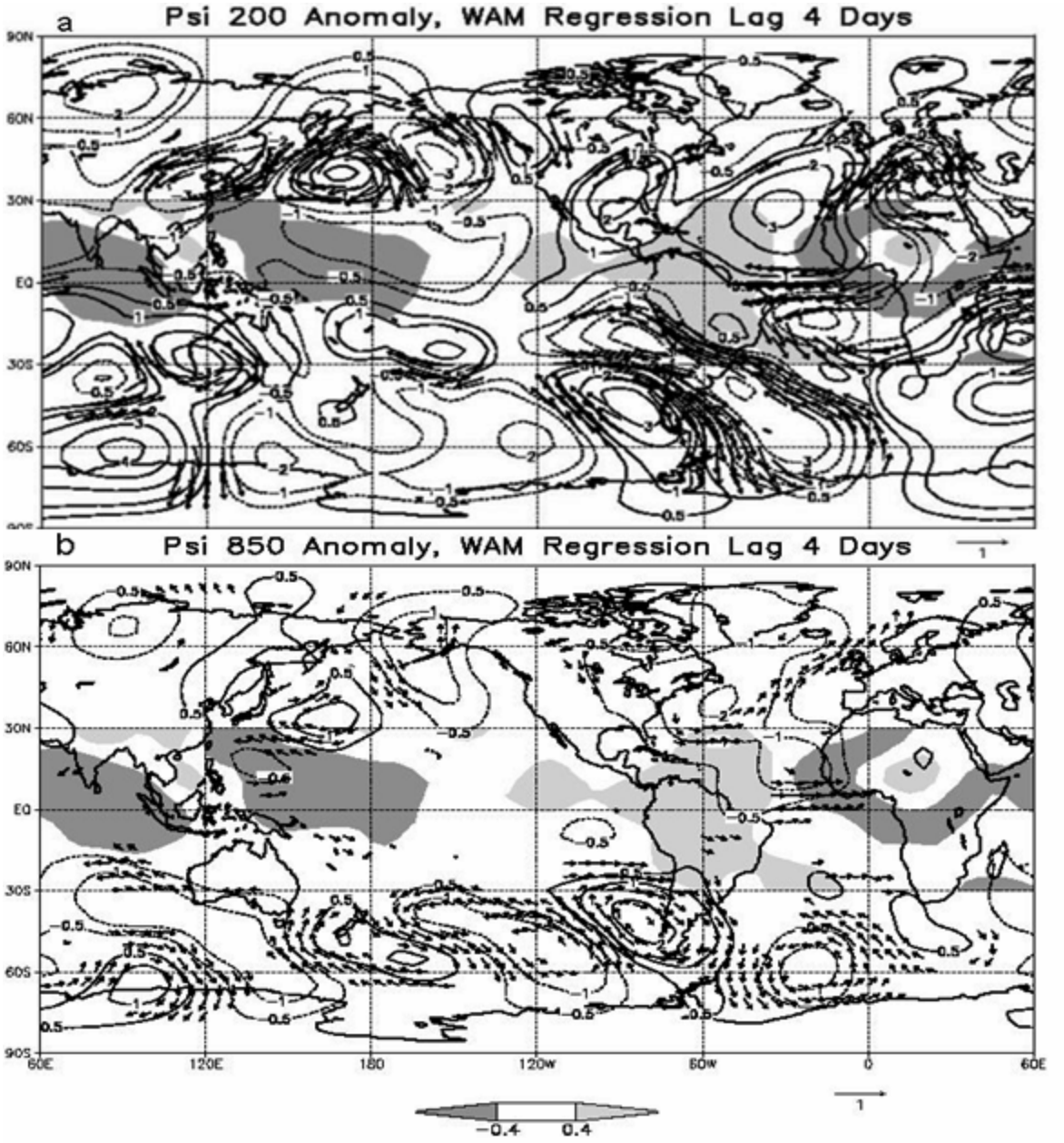


Figure 3.17 As in Figure 3.15, except for lag +4 days.

### *d. Summary*

At upper levels, the regression of streamfunction based on OLRA over western Africa contains wave train -like features similar to those found in the regression maps based on zonal wind over the equatorial Atlantic. However, the regression based on OLRA defined more of a signal in the NH.

At low levels, the SH wave train pattern in the OLRA based regression maps was not as well defined as found in the regression maps based on the zonal wind anomalies. Rather, the low-level streamfunction pattern seems to resemble the circulation response to heating over western Africa, as cyclonic anomalies that straddle the equator over the equatorial Atlantic seem to be most responsible for the equatorial westerly wind anomalies.

## 4. E-Vector Analysis

The wave propagation characteristics defined by the series of regression maps are examined using **E**-vectors computed over the period from -8 days to +8 days. Areas of **E**-vector convergence reflect areas of increasing eddy kinetic energy (Hoskins et al. 1983). Alternatively stated, **E**-vector convergence indicates areas where the transient eddies are acting to decelerate the mean flow (Kiladis 1998).

The **E**-vectors pattern associated with the regression based on the zonal wind index (Figure 3.18) define equatorward-propagating wave activity over the South Atlantic. An area of significant eddy growth, denoted by the strong convergence of the **E**-vectors, extends meridionally along approximately 40°W, between 60°S to 30°S. Over the equatorial south Atlantic, the **E**-vectors turn westward, which indicates that there is no cross-equatorial propagation as eddies that reach this area are becoming zonally elongated.

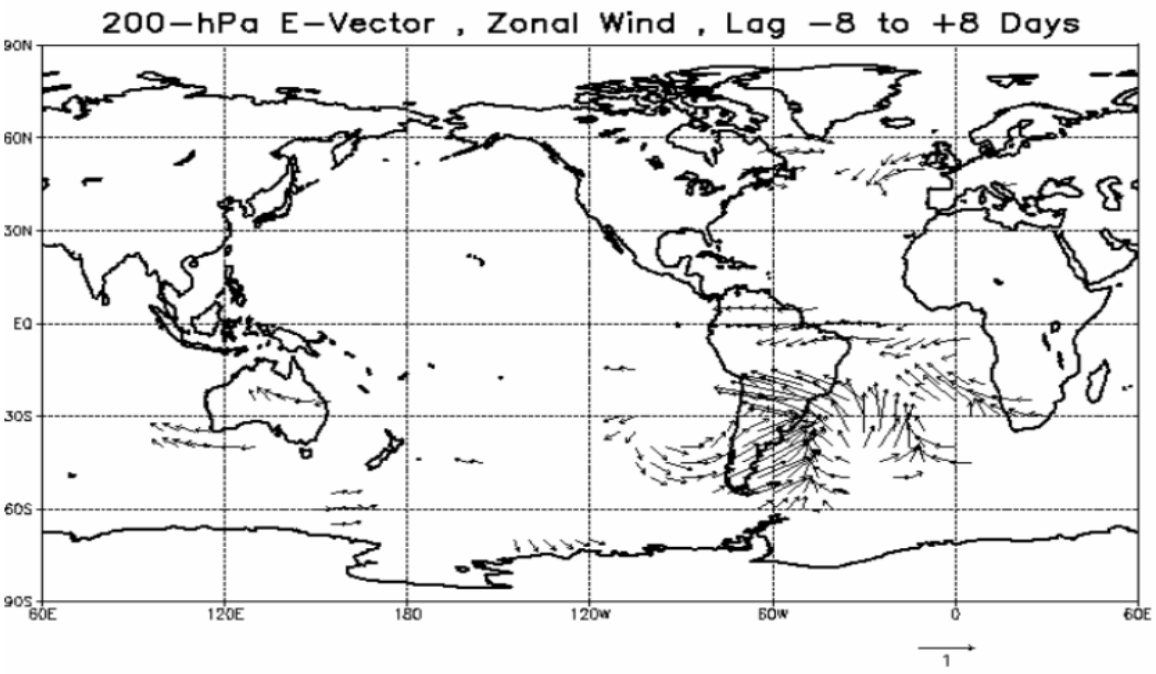


Figure 3.18 Mean 200-hPa **E**-vectors ($m^2 s^{-2}$) from day -8 to day +8 for the regression based on the anomalous zonal wind in the tropical Atlantic. Reference vector is located in the bottom right.

An examination of the **E**-vector plot associated with the regression based on the OLRA index in West Africa (Figure 3.19) defines equatorward-propagating features with similar characteristics over the South Atlantic. However, over the NH, the **E**-vectors indicate the presence of midlatitude wave propagation across North America that appears to be originating in the North Pacific jet. Once this wave reaches the east coast of North America, there is a decided equatorward bend.

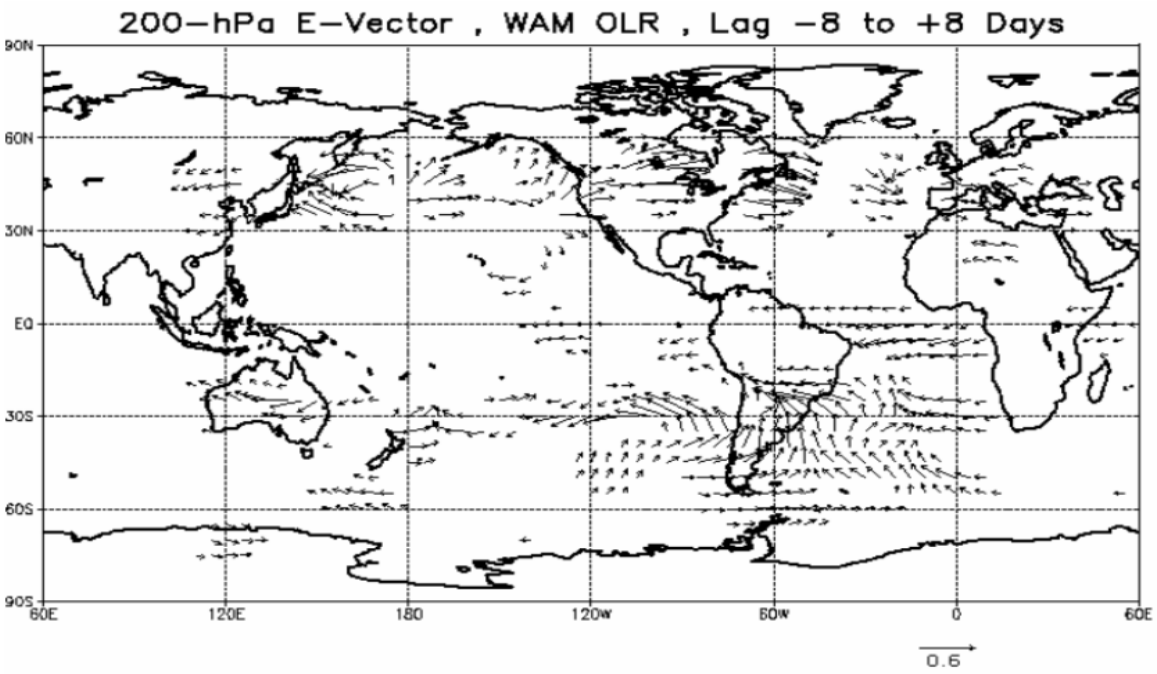


Figure 3.19 As in Figure 3.18, except for the regression based on the OLR anomalies associated with the WAM.

## D. INTERANNUAL VARIABILITY OF THE COUPLED CIRCULATION EVENTS

### 1. Background

The relative spatial and temporal relationships among the base indices and the wind and OLRA fields are described by the regression analysis. A maximum in westerly zonal wind anomalies across the equatorial Atlantic appears several days following a negative OLRA over western Africa. Also, there is a lagged relationship between large cyclonic anomalies west of Chile at 850 hPa and the occurrence of positive zonal wind anomalies over the equatorial Atlantic. A measure of the strength of the cyclonic anomaly near Chile is computed by the area average 850-hPa streamfunction anomaly over 75°W-105°W, 45°S-60°S. The relationships are examined by the considering time series of each parameter for each May-October period between 1979 and 2001. To relate these parameters to low-level wave activity in the tropical Atlantic, the square of the 850-hPa meridional wind is computed as a measure of wave activity.

To strictly define a significant event, the following requirements were adopted:

1) The OLRA index and the zonal wind anomaly index must have a near quadrature relationship
2) The OLRA index must lead the zonal wind anomaly index
3) The leading OLRA and the following zonal wind anomaly maximum must both be greater than one standard deviation above their respective means.

Once an event is located in time, the variance of the meridional wind and the value of streamfunction off the coast of Chile are then evaluated relative to each event.

**2. Time Series Analysis**

Specific cases that occurred during the first five years of the analyzed time series (Figure 3.20) are highlighted by a thick box surrounding the approximate timing of the event. The shading in the plots indicates anomalies greater than the respective mean plus one standard deviation. The vertical bars indicate formation dates and relative locations of TC formations in the tropical Atlantic as defined in the best-track data. A vertical bar in the positive region indicates a formation in the tropical Atlantic, between the longitudes of 35°W and 60°W, while a vertical bar in the negative region indicates a formation between 10°W and 35°W.

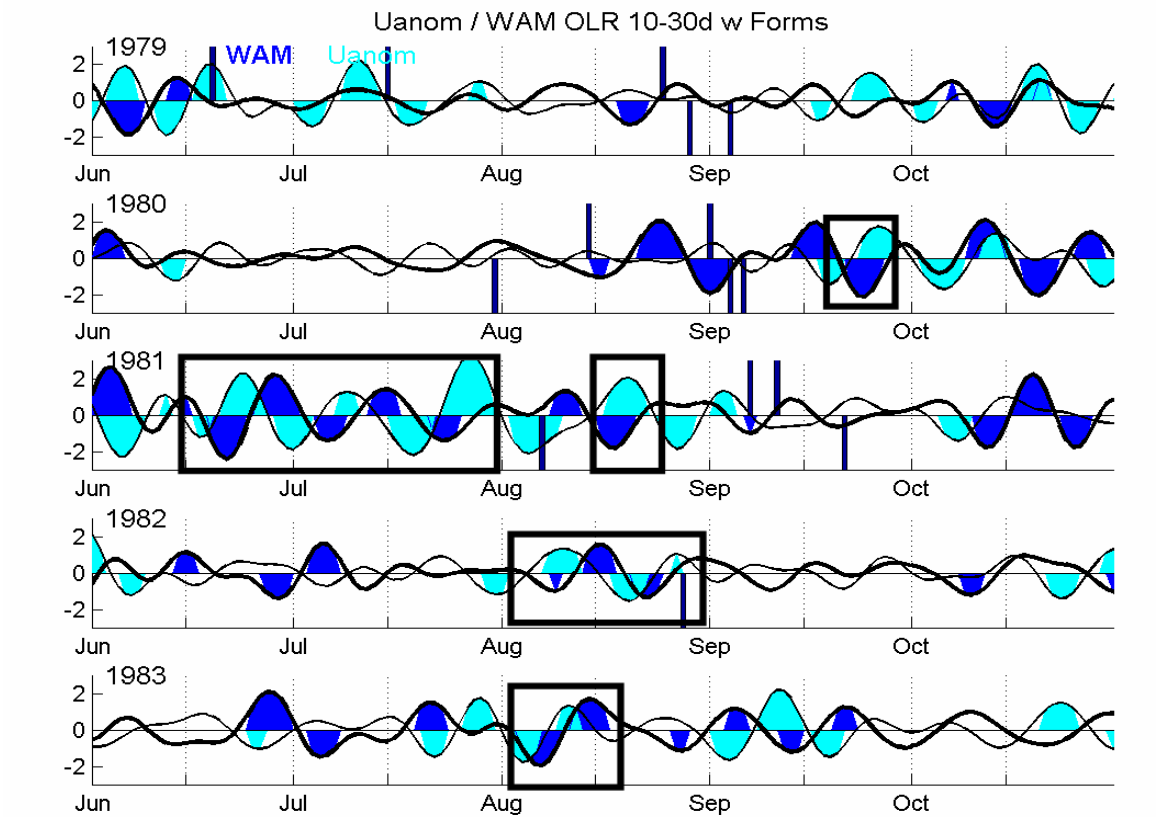


Figure 3.20 Time series of OLRA index over West Africa, zonal wind anomaly over the tropical Atlantic, and TC formations for the years indicated on the plot. Values are normalized anomalies (unitless, mean of zero, and unit variance). TC formations are depicted by the vertical bars (see text for details of plotting convention).

A set of cycles begins on approximately 15 June 1981 and continues until approximately 1 August 1981. The length of 45 days defines an approximate period of 15 days for each cycle. This set of cycles serves as the basis for the composite charts presented in Chapter 3, section D, subsection 3.

Using the times indicated by the boxes as reference, similar plots that include the 10-30 day filtered 850-hPa anomalous streamfunction off the west coast of Chile (Figure 3.21) and the variance of the 850-hPa meridional wind [not plotted as a normalized anomaly] are analyzed to determine how often these coupled midlatitude/tropical Atlantic events occur.

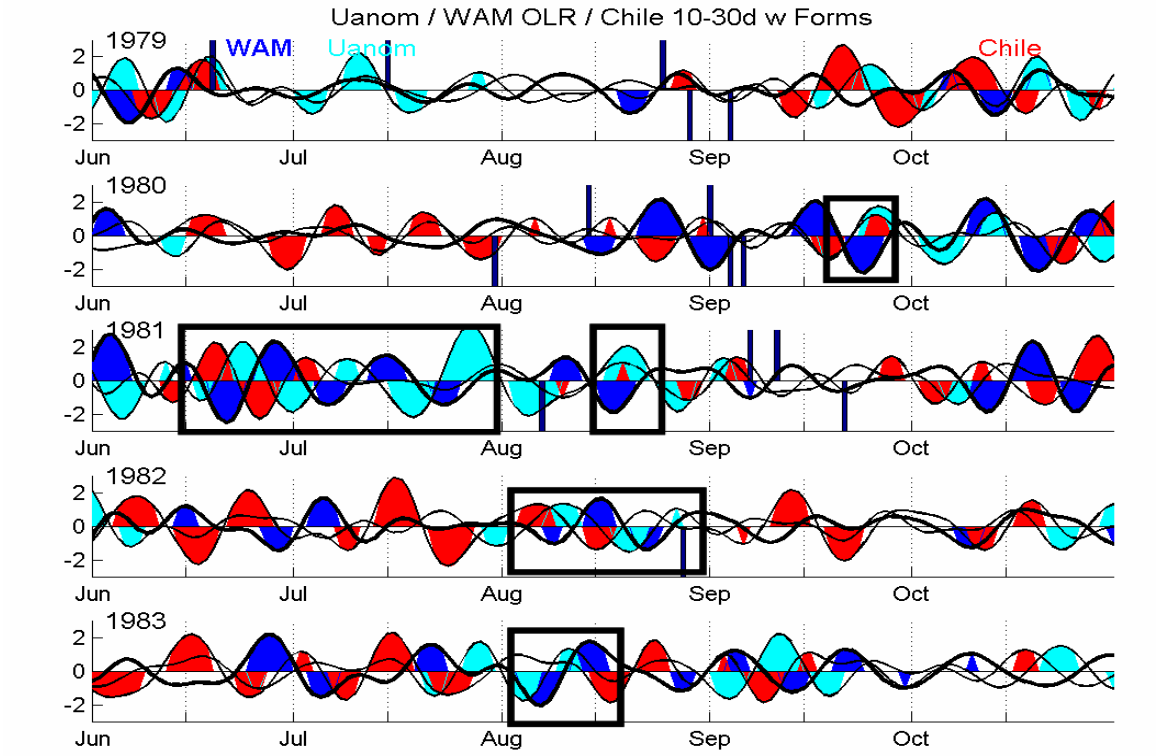


Figure 3.21 Similar to Figure 3.20, except that index measuring wave activity near Chile has been added.

For the 1981 case, (Figure 3.22) it can be seen that a significant cyclogenesis event occurs around 20 June 1981, several days later a convective maximum occurs over Africa, and several days later a zonal wind anomaly maximum occurs in the tropical Atlantic. The pattern then repeats, with all of the indices going through periodic cycles as indicated in the entire regression sequence.

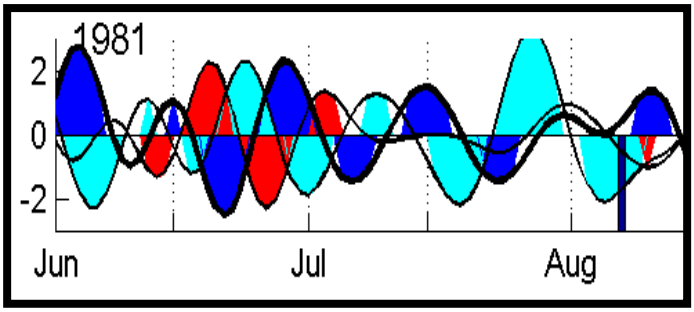


Figure 3.22 Time series of OLRA in West Africa (blue), zonal wind anomaly in the tropical Atlantic (cyan) and 850-hPa streamfunction west of Chile (red) for the period 1 Jun – 15 Aug 1981.

To identify a link with potential TC formation over the tropical Atlantic, the relationship between these events and wave activity in the tropical Atlantic is examined (Figure 3.23). For most events, a statistically significant peak in wave activity is realized during or just slightly after the peak in equatorial westerlies, which suggests that the increased background vorticity contributes to the growth of low-level waves propagating into the region. It should be noted that not all events result in significant wave activity.

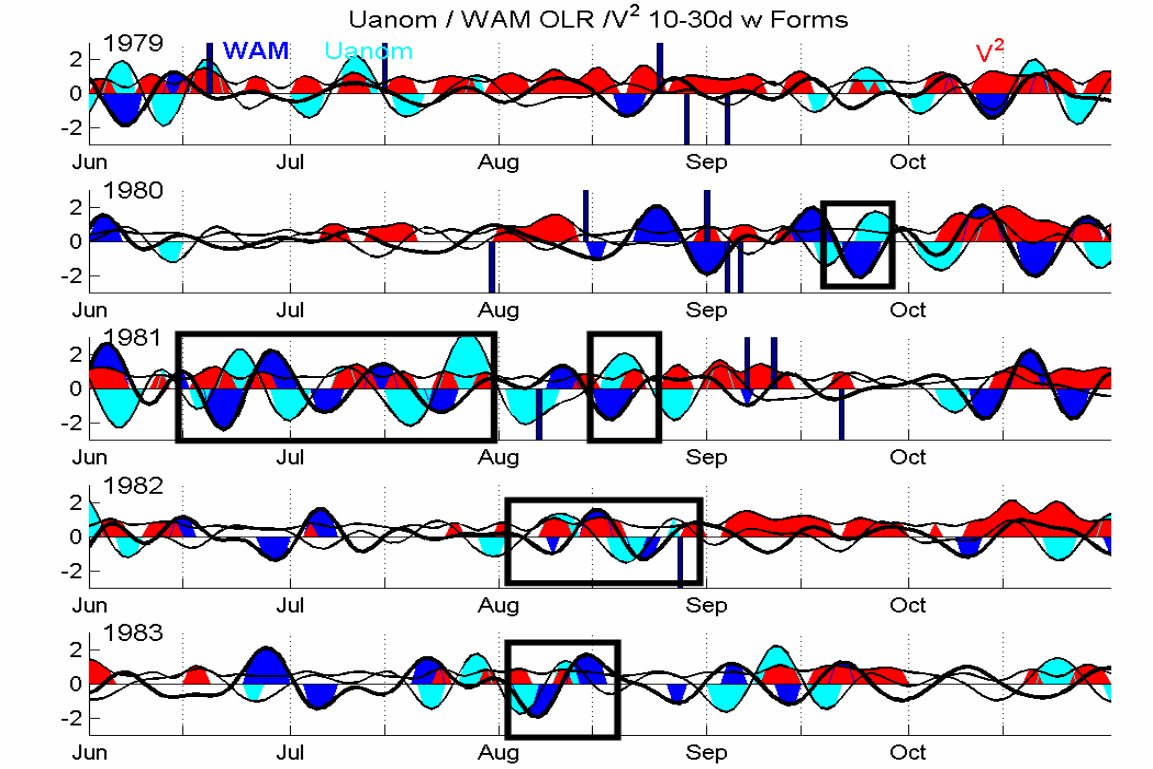


Figure 3.23 Similar to Figure 3.21, except that the index for the variance of the meridional wind ($v^2$) has been added. The variance is normalized by dividing by the standard deviation of the data, but no mean is subtracted.

While the main source of wave activity in this region can be attributed to African easterly waves (AEWs), which for most of their life cycle have peak amplitude at the level of the African Easterly Jet (AEJ), once the AEWs move over the waters of the eastern Atlantic, the strongest wave activity typically shifts to lower levels, where there cyclonic vorticity is maximized (Thorncroft and Hodges 2001).

Summary statistics for all of the years analyzed in this study (Table 1) show that most (76%) of the occurrences of zonal wind anomaly/OLRA events are associated with increased wave activity. The additional time series plots, for all years up to 2000, are included in the Appendix.

| Year | U' & OLRA Events | U' & OLRA Events with significant V2 | % of events with significant V2 | Total TC Formations | TC Formations in U'/OLR' event | TC Formation in U' / OLRA / $V^2$ event | % TC in U' / OLRA / $V^2$ event |
|---|---|---|---|---|---|---|---|
| 1979 | 1 | 1 | 100.00 | 5 | 0 | 0 | 0.00 |
| 1980 | 2 | 0 | 0.00 | 5 | 0 | 0 | 0.00 |
| 1981 | 5 | 5 | 100.00 | 4 | 0 | 0 | 0.00 |
| 1982 | 2 | 2 | 100.00 | 1 | 1 | 1 | 100.00 |
| 1983 | 1 | 1 | 100.00 | 0 | 0 | 0 | No TC |
| 1984 | 2 | 2 | 100.00 | 3 | 0 | 0 | 0.00 |
| 1985 | 5 | 4 | 80.00 | 1 | 0 | 0 | 0.00 |
| 1986 | 1 | 1 | 100.00 | 1 | 0 | 0 | 0.00 |
| 1987 | 2 | 1 | 50.00 | 4 | 0 | 0 | 0.00 |
| 1988 | 2 | 2 | 100.00 | 6 | 0 | 0 | 0.00 |
| 1989 | 2 | 2 | 100.00 | 7 | 1 | 1 | 14.29 |
| 1990 | 3 | 2 | 66.67 | 8 | 2 | 2 | 25.00 |
| 1991 | 5 | 4 | 80.00 | 1 | 1 | 1 | 100.00 |
| 1992 | 2 | 2 | 100.00 | 1 | 0 | 0 | 0.00 |
| 1993 | 2 | 2 | 100.00 | 4 | 0 | 0 | 0.00 |
| 1994 | 3 | 2 | 66.67 | 3 | 0 | 0 | 0.00 |
| 1995 | 2 | 1 | 50.00 | 9 | 1 | 1 | 11.11 |
| 1996 | 4 | 3 | 75.00 | 6 | 3 | 2 | 33.33 |
| 1997 | 4 | 1 | 25.00 | 1 | 0 | 0 | 0.00 |
| 1998 | 2 | 1 | 50.00 | 7 | 0 | 0 | 0.00 |
| 1999 | 3 | 3 | 100.00 | 5 | 2 | 1 | 20.00 |
| 2000 | 1 | 1 | 100.00 | 7 | 2 | 0 | 0.00 |
| TOTAL | 56 | 43 | 76.79 | 89 | 13 | 9 | 10.11 |

Table 1. Summary statistics for the relation of U' (850-hPa zonal wind anomaly) / OLRA in West Africa events with wave activity ($V^2$) and TC formation in the tropical Atlantic.

### 3. Relation of Zonal Wind Anomaly/OLRA Events to TC Formations

While the link between zonal wind anomaly/OLRA events and wave activity is strong, the relationship between zonal wind anomaly/OLRA events that contain significant wave activity and overall TC formation is not robust. This can be seen by examining the last four columns of Table 1. Nearly 77% of all zonal wind/OLRA events contain significant wave activity, yet only 69% of all TCs that formed during a zonal wind/OLRA anomaly event are associated with increased

wave activity. Furthermore, only 10% of all TC formations in the tropical Atlantic are associated with an event that contains significant wave activity.

The lack of a direct connection may be explained by the results of Thorncroft and Hodges (2001), which posits that the strength of the AEWs in the low-levels as each wave exits the coast of Africa, is a critical factor in determining if the AEW will develop into a TC. That topic is not addressed in this study.

It may also be explained by examination of regression maps based on vertical shear in the tropical Atlantic (Figure 3.24). The regression based on the vertical shear of the zonal wind is scaled according to a value of shear that is one standard deviation below the mean, representing significant easterly shear. A period of significant easterly shear tends to represent a time period when the upper-level westerlies are far away from the tropical Atlantic. In addition, considering only the zonal component of the wind allows the shear to be represented by a single variable, and is justified because in the tropical Atlantic the zonal shear is very highly correlated with the total shear (DeMaria 1999).

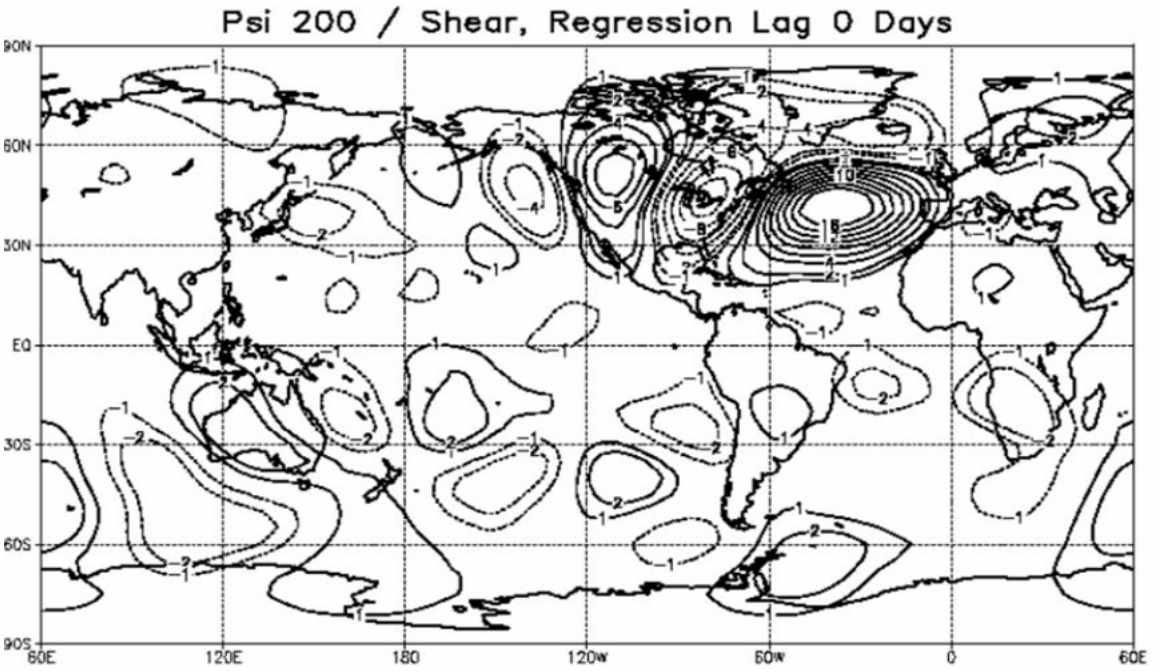


Figure 3.24 200-hPa streamfunction anomalies in the 10-30-day band during June-Oct 1979-2001 that are associated with a value of the 200-850-hPa anomalous shear of zonal wind that is one standard deviation below the mean in the region 0-20°N, 60°W-10°W. A simultaneous regression is depicted.

The regression maps confirm that changes in shear in the tropical Atlantic are strongly linked to the intrusion of NH midlatitude circulations. Therefore, it may be that a combination of the correctly phased parameters in *both* Northern and Southern Hemispheres may give rise to the most favorable dynamic conditions for TC formation on the intraseasonal time scales on which this study focused.

## E. CASE STUDY

### 1. Background

To more fully examine the relationship of 200-hPa, midlatitude circulation anomalies to the coupled wind-convection patterns in West Africa, composite charts are used to illustrate the events that occur from approximately 15 June 1981 to 1 August 1981. As defined in the previous section, the events in this time period are associated with strong wave activity in the South Pacific and increased wave activity in the tropical Atlantic, but no TC formations.

For the time period from 15 June- 1 August, we retained the dates of critical values of the zonal wind anomaly and OLRA indices. Phase 0 was associated with the day of the maximum westerly zonal wind anomaly (Figure 3.25). Phase -1 represents the day of the immediately preceding zero crossing of the zonal wind anomaly index, where the anomalous winds transition from easterly to westerly. Phase -2 represents the day of the maximum easterly wind anomaly that precedes Phase -1. Phase +1 is associated with the zero crossing immediately following the westerly wind anomaly maximum, and Phase +2 represents the following easterly wind anomaly. For multiple, repeated cycles, Phase +2 of the earlier event and Phase -2 of the adjacent following event would represent the same day. Composite charts constructed based on the WAM index are based on inverse relation of Phase number to value of the OLRA index described above, i.e., Phase 0 for the WAM represented a minimum in OLRA values and Phases -2 and +2 represent maximum values of OLRA.

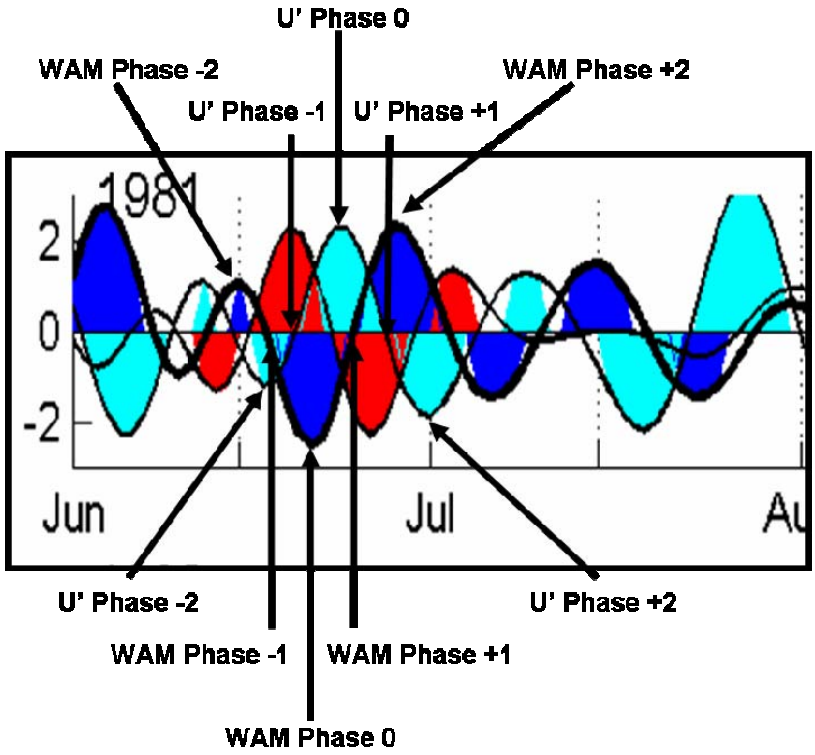


Figure 3.25 Sample of time series chart used to identify significant values associated with related cycles of the 850-hPa zonal wind anomaly in the tropical Atlantic as coupled with the OLR anomaly in the WAM. Individual days are referred to as Phases. U' indicates the anomalous zonal wind.

## 2. Composite Charts

### *a. Phase -2*

At Phase -2 for the WAM OLRA index, the 200-hPa anomalous circulations (Figure 3.26) indicate the presence of significant wave trains in both hemispheres that appear to be related to source regions in the western and central Pacific. The SH wave train crosses South America and then turns equatorward over the South Atlantic.

The forcing for these wave trains appears to be two-fold. One region of forcing appears to be convection in the Maritime Continent region, as indicated by negative OLR anomalies extending along approximately 10°N from near Vietnam to near 150°W. A smaller area of convection is also present east of Papua New Guinea. Another area of convection in the equatorial Central Pacific also appears to be forcing anomalous circulations that propagate into the

midlatitudes. The wave trains excited by these convective regions interact in the eastern North Pacific and eastern South Pacific, where they combine into the wave trains described in the previous paragraph.

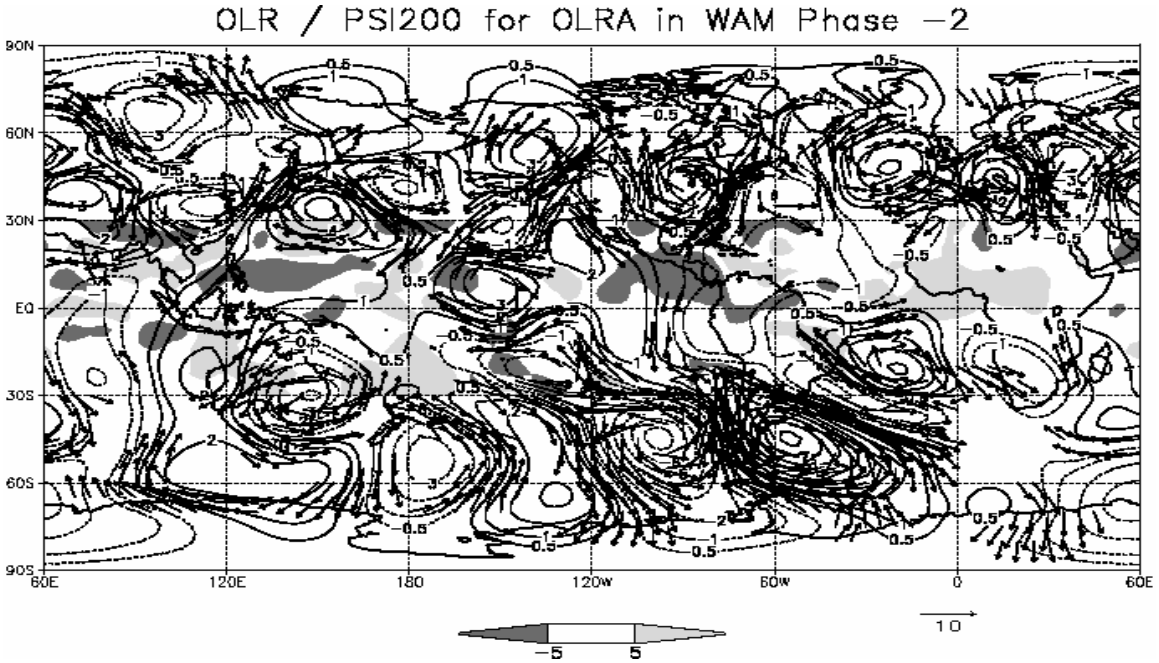


Figure 3.26 Composite chart for Phase -2 based on the OLRA in WAM for summer 1981 showing 200-hPa streamfunction, winds (>3 m $s^{-1}$), and OLRA. All quantities are time filtered to retain the 10-30-day band. See text for definition of Phases. Reference vector is in the bottom right.

The 200-hPa anomalous circulations associated with Phase -2 of the 850-hPa zonal wind anomaly index (Figure 3.27) closely resemble those associated with Phase -2 of the WAM index with few exceptions. For the time period about which these composite charts are generated, it should be noted that Phase -2 in the zonal wind anomaly index occurs 2-4 days after Phase -2 of the WAM index. Over the SH, the composite chart indicates that the circulation anomalies have an eastward component of propagation. Anomaly centers over the western South Pacific also have a poleward component of propagation, while eddies east of South America have a distinct northwest-southeast tilt, indicating continued equatorward propagation.

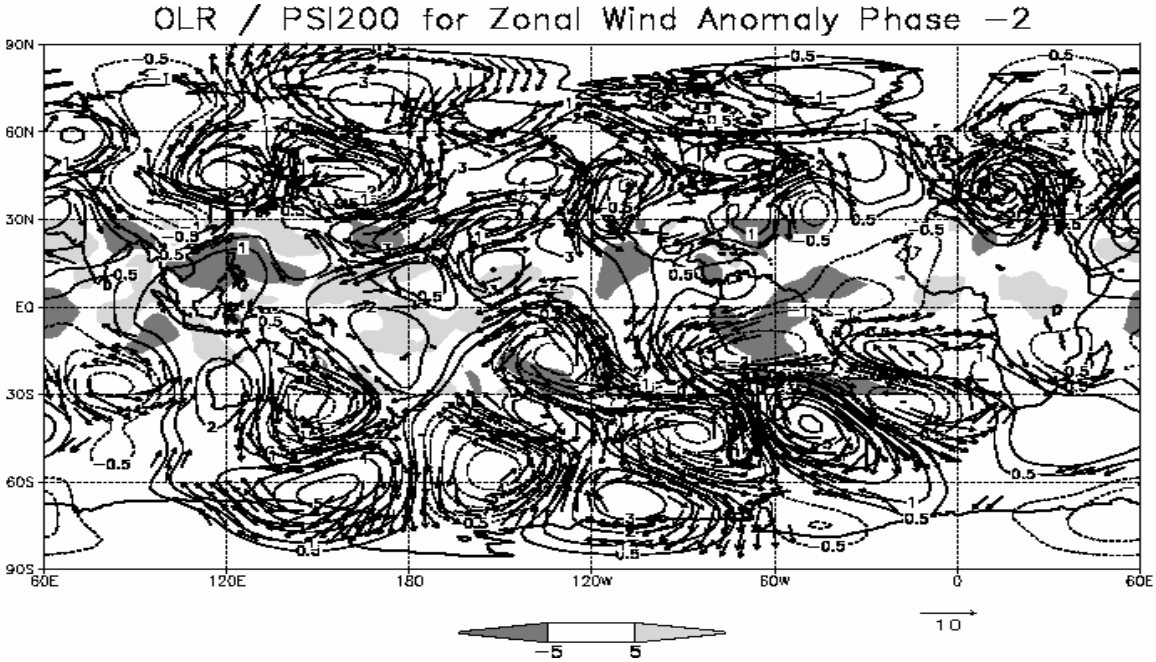


Figure 3.27 Composite chart for Phase -2 based on the zonal wind anomaly in the tropical Atlantic for summer 1981 showing 200-hPa streamfunction, winds (>3 m $s^{-1}$), and OLRA. All quantities are time filtered to retain the 10-30-day band. See text for definition of Phases. Reference vector is in the bottom right.

### *b. Phase -1*

As the WAM index approaches zero, Phase -1 (Figure 3.28), the circulations present at 200-hPa are similar to those present at Phase -2 of the zonal wind anomaly index. This is not surprising, due to the near quadrature relationship of the two indices. The most prominent feature is a high amplitude wave train that extends from the SH midlatitudes to the equatorial South Atlantic. A cyclonic anomaly associated with this wave train is located in the equatorial South Atlantic. Assuming a baroclinic structure in the tropics (Kiladis and Weickmann 1997), this would place an anticyclone circulation in the low-levels, and result in increased, cross-equatorial flow from the ocean to the land in West Africa.

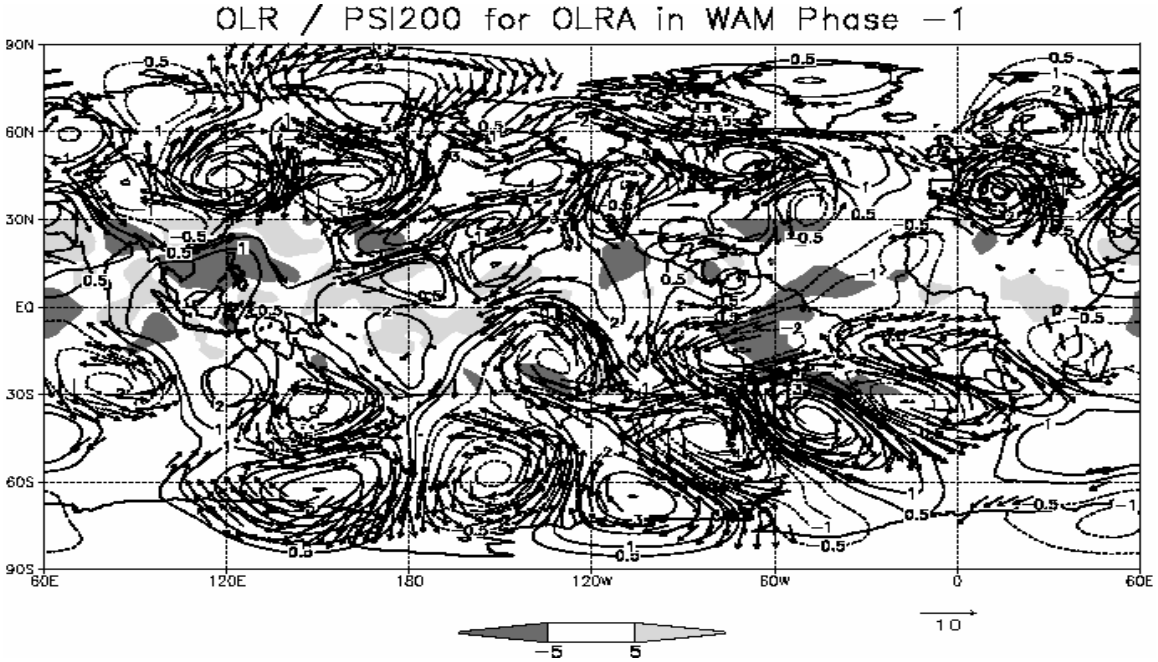


Figure 3.28 As in Figure 3.26, except for WAM Phase -1.

The upper-level structure associated with Phase -1 of the zonal wind anomaly (Figure 3.29) reinforces a direct connection from the central Pacific to the South Atlantic via the SH wave train. Concurrent with a reduction in the coverage of negative OLRAs over Southeast Asia from zonal wind anomaly Phase -2 to Phase -1, a direct connection with the western Pacific is no longer seen.

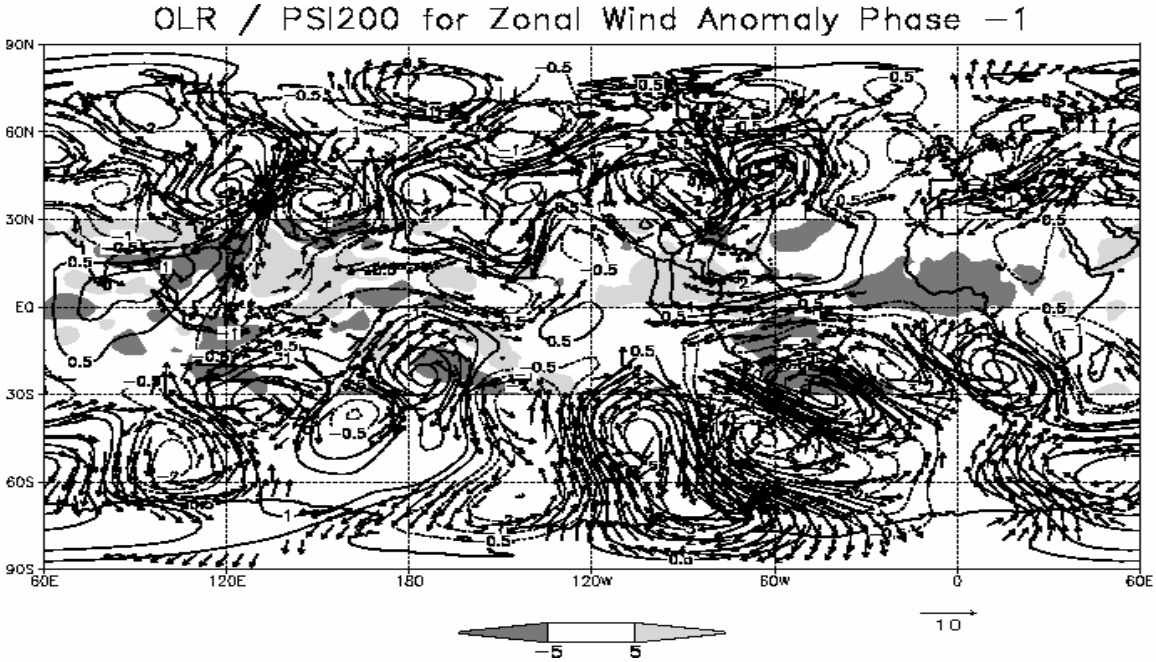


Figure 3.29 As in Figure 3.27, except for zonal wind anomaly Phase -1.

### *c. Phase -0*

The pattern related to Phase 0 in the WAM index (Figure 3.30), is very similar to the pattern related to Phase -1 of the zonal wind anomaly. A strong wave train in the SH midlatitudes, which exhibits equatorward propagation in the South American region, is still present. An anticyclonic anomaly is moving into the South Atlantic, with easterly winds to the west of the convection.

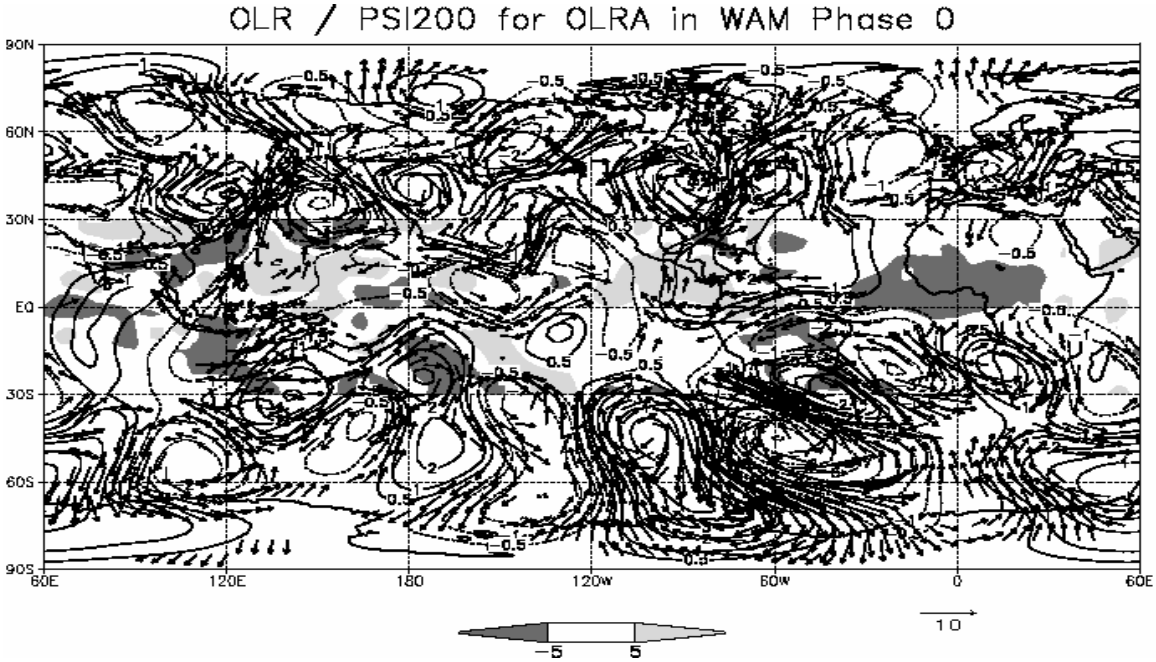


Figure 3.30 As in Figure 3.26, except for WAM Phase 0.

The 200-hPa circulations related to Phase 0 of the zonal wind anomaly index (Figure 3.31) are opposite in sign from those present at Phase -2. Easterly wind anomalies are now found over the equatorial South Atlantic in response to an anticyclonic anomaly located at approximately 15°S, 20°W. As compared to the OLR anomaly over West Africa in Phase 0 based on the WAM index, the negative OLR anomaly over West Africa has contracted. The average spacing in time between WAM Phase 1 and U' Phase 1 is 3 days.

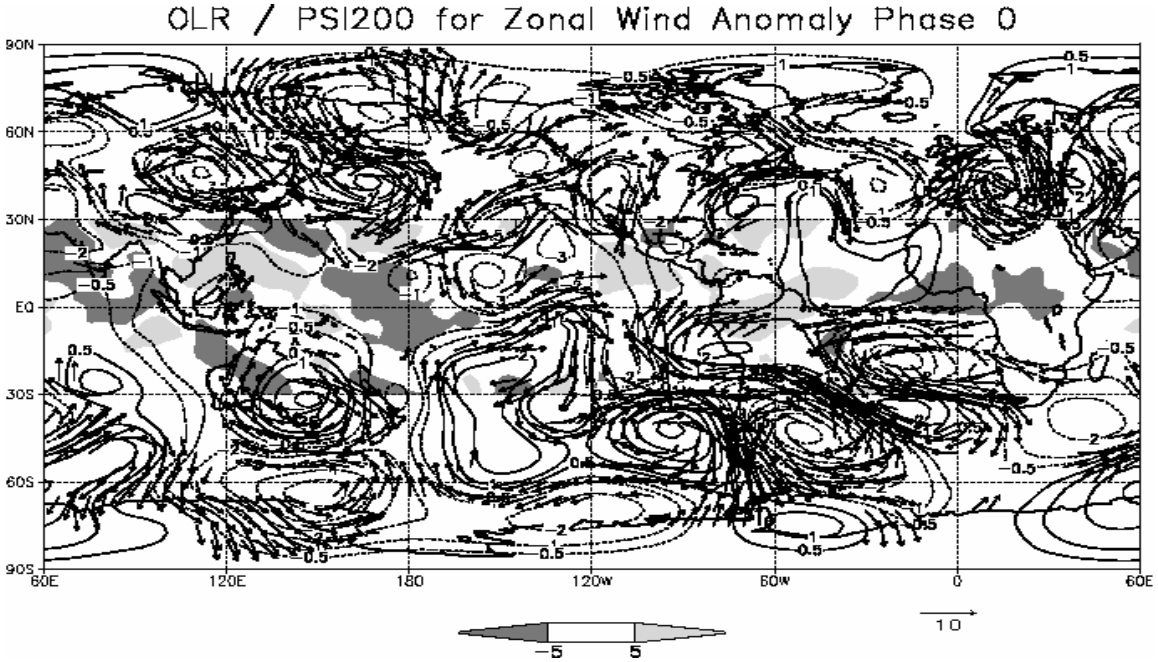


Figure 3.31 As in Figure 3.27, except for zonal wind anomaly Phase 0.

### *d. Phase +1*

The 200-hPa anomalous circulations for the day indicated by Phase 1 in the WAM index (Figure 3.32) indicate the presence of a prominent wave train in the SH midlatitudes that extends from the central South Pacific to Sub-Saharan Africa. In the region between a cyclonic circulation over the Amazon Basin and an anticyclonic circulation over the South Atlantic, there is a lull in the upper-level winds over the equatorial Atlantic. The reduced spatial extent of the OLRAs over West Africa indicates a continued weakening of the convection associated with the WAM.

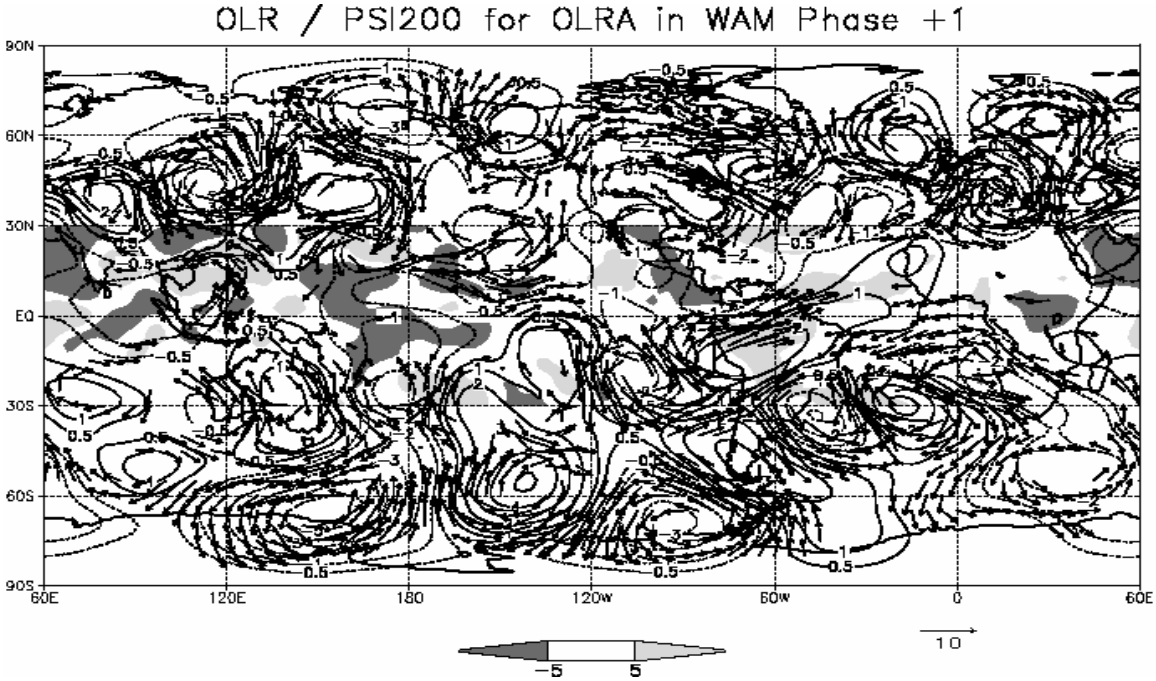


Figure 3.32 As in Figure 3.26, except for WAM Phase +1.

At Phase 1 of the zonal wind anomaly index (Figure 3.33) the midlatitude wave trains in both hemispheres have zonal orientations over the Atlantic, and no longer appear to have a large impact on the winds in the equatorial Atlantic. The SH wave train maintains a connection to the central Pacific via an anticyclonic anomaly at 20°S, 170°W. At Phase -1 for the zonal wind anomaly, a cyclonic circulation of similar magnitude existed in the same location. In association with reduced convection in the WAM, the development of a small, anticyclonic anomaly near the coast of Africa around 20°N, is similar to the results obtained by Sultan et al. (2003).

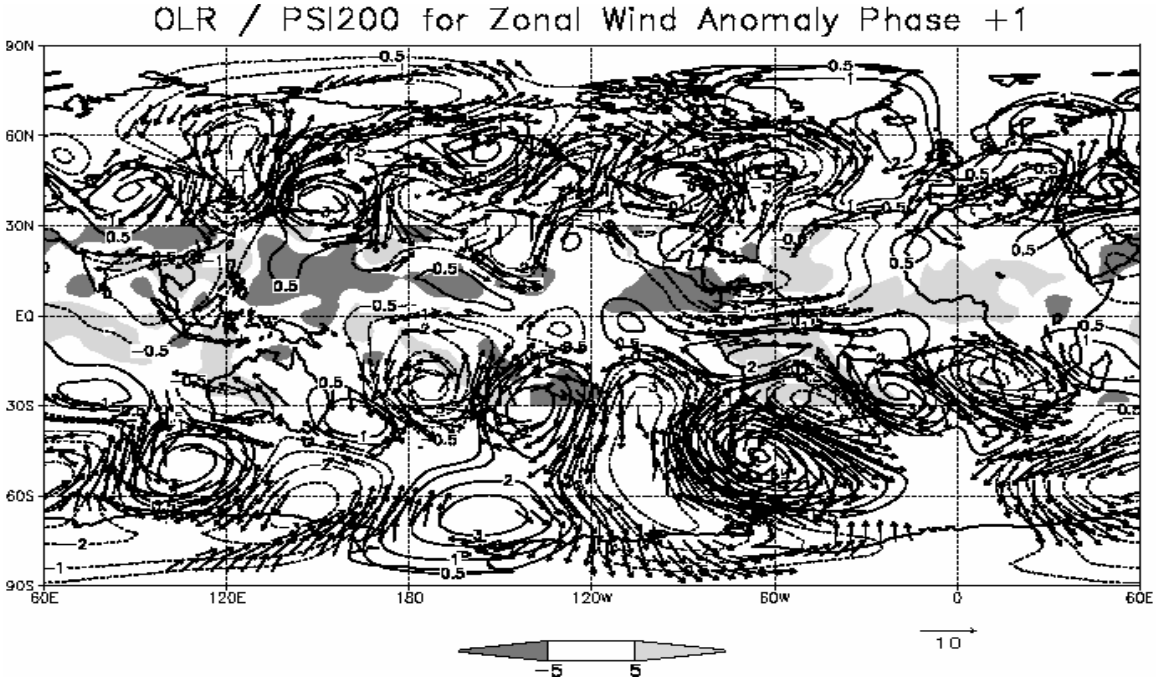


Figure 3.33 Similar to figure 3.27, except for zonal wind anomaly Phase +1.

### *e. Phase +2*

The 200-hPa circulation pattern for Phase +2 of the WAM index (Figure 3.34) very closely resembles that of Phase -2, with the exception of an easily recognizable connection to West Pacific convection. There are still indications of connections to central Pacific convection, and to the higher latitudes of the SH at approximately 150°W. As in Phase -2, the SH wave train turns equatorward over the South Atlantic, and beings to impart westerly wind anomalies at the upper-levels over the equatorial Atlantic.

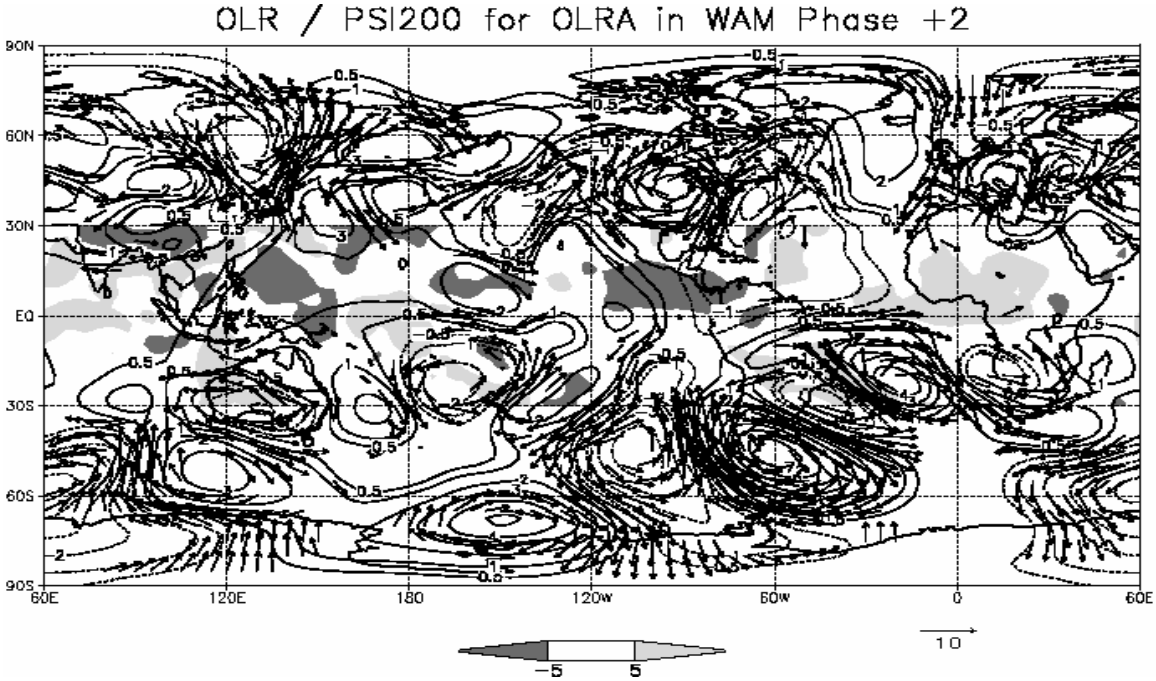


Figure 3.34 Similar to figure 3.26, except for WAM Phase +2.

Many of the upper-level features associated with Phase +2 of the zonal wind anomaly index (Figure 3.35) show a close relation with those present at Phase -2. The circulation anomalies in the SH that lie between 120°W and Africa are similar to those present at the earlier phase. The similarities between Phase -2 and Phase +2 in the NH are less obvious. The areas showing the least amount of similarity are the North Pacific, Asia and Indian Ocean. Many features in these regions at Phase -2 have no comparable feature at Phase +2, indicating that after the time period indicated by Phase +2, the atmosphere may be responding to different forcing mechanism than during Phase -2.

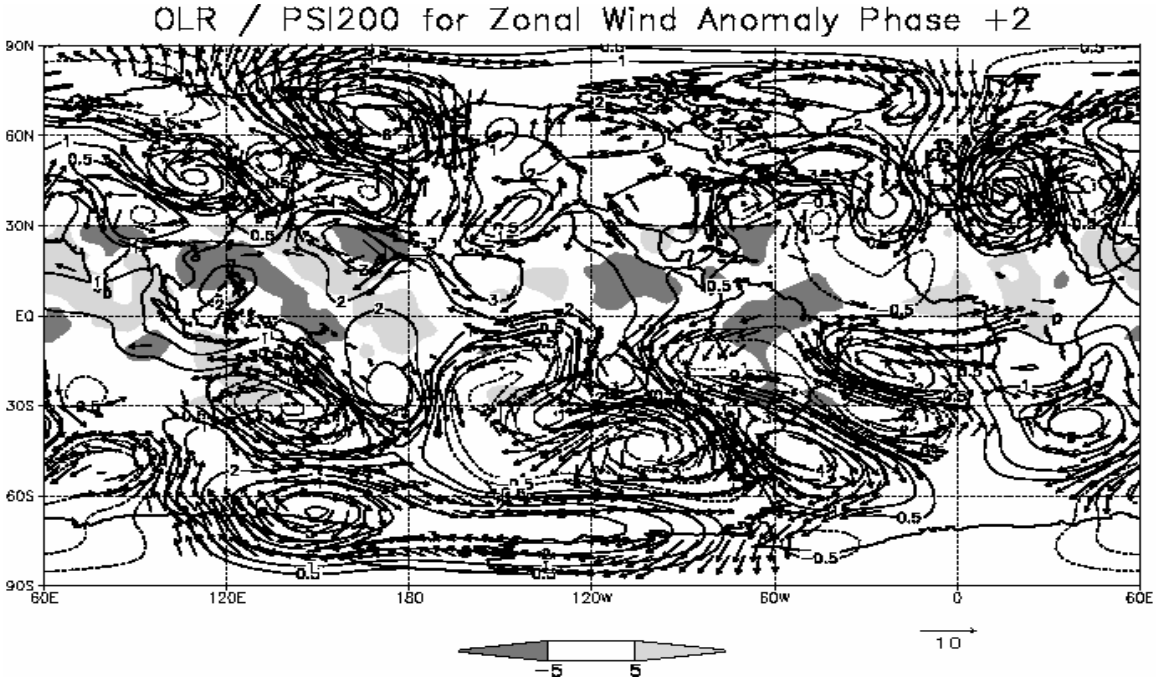


Figure 3.35 Similar to figure 3.27, except for zonal wind anomaly Phase +2.

# IV. SUMMARY AND CONCLUSION

## A. SUMMARY

Burton (2005) examined intraseasonal oscillations in the SH midlatitudes that, in combination with intraseasonal oscillations in the tropical western Pacific, enhanced (or suppressed based on the cycle) convection in the tropical western North Pacific monsoon trough. He identified significant structures that are present in the large-scale circulation patters of the SH, and related the anomalous Rossby-wave associated variability in these structures to the cycles of convection identified by Delk (2004).

In studies comparable to that conducted by Delk (2004), Sultan et al. (2003) and Grodsky and Carton (2001) linked significant intraseasonal rainfall and convective variability over the equatorial Atlantic and West Africa with variations in the wind field associated with the tropical Atlantic-West African monsoon circulation system. This purpose of this study was to examine the characteristics of SH, midlatitude wave activity that could have a connection to the previously detailed variability in the tropical Atlantic-WAM circulation system.

Further analysis of EOF 2 and EOF 3 of 700-hPa height anomalies identified a possible source of wave activity in the SH midlatitudes and a preferred path of propagation into the Atlantic. EOF 2 and EOF 3 comprise a single mode, which is characterized by a large-scale Rossby-wave train with maximum amplitude in the South Pacific and evidence of equatorward propagation in the South Atlantic. In addition to identifying this source of wave activity, it was shown that significant wave activity in the SH midlatitudes occurs on approximately the same intraseasonal time scales as variations in the tropical Atlantic.

To objectively define the relationship between the wave activity that propagates through the SH midlatitudes and the downstream effects on the tropical Atlantic-West African monsoon circulation system, linear regression analyses based on critical variables in the target regions were conducted.

SH midlatitude circulations strongly impacted the 850-hPa vorticity and convection over the region of the West African monsoon. According to the results of the linear regression analysis study, a significant cyclonic anomaly off the west coast of Chile, at approximately 90°W, is related to a wave train that propagates along an approximate great circle route from the South Pacific to the tropical Atlantic. A few days later, an anticyclonic anomaly associated with this wave train reaches the equatorial Atlantic, causing easterly anomalous winds in the tropical Atlantic and enhancing convection with increased cross-equatorial flow that carries moist air over the land areas of West Africa. As the wave train propagates equatorward over the tropical Atlantic, the low-level anticyclonic anomaly is replaced by a cyclonic anomaly that contributes to a westerly zonal wind anomaly over the equatorial Atlantic. The anomalous westerly wind coincides with enhanced convection that moves from western Africa toward the Atlantic Ocean.

Additionally, an inspection of indices representing the submonthly component of the anomalous low-level zonal wind in the tropical Atlantic, wave activity in the tropical Atlantic, convective activity associated with the West African monsoon, and midlatitude wave activity in the South Pacific was used to define time periods when significant circulation anomalies in the SH midlatitudes were linked to circulation and convection anomalies in the tropical Atlantic. It was shown that a large part of the intraseasonal variance in tropical Atlantic wave activity can be explained by links to perturbations in the South Pacific, but the relationship of intraseasonal South Pacific wave activity with variability in TC formation in the tropical Atlantic was not nearly as strong.

In part, the lack of a clear relationship with TC activity is due to interference from other factors that affect TC formation. For example, NH midlatitude circulations were shown to affect deep layer vertical shear in the tropical Atlantic and convection in West Africa through the intrusion of midlatitude troughs and ridges. The intrusion of a midlatitude trough into the tropical Atlantic would bring increased westerly shear, while the development of an anticyclone over the North Atlantic would bring favorable, easterly shear to the region.

Composites of three, back-to-back cycles of significant South Pacific wave activity followed by increased convective activity in West Africa and then by increased wave activity in the tropical Atlantic confirmed the results of the regression analysis.

The overall result of this study shows that on submonthly time scales, a constructive combination of circulation in both the northern and southern hemispheres is critical for developing favorable conditions in the dynamic quantities that influence the probability of TC formation.

## B. FUTURE WORK

Based on this study, on the submonthly time scale a significant connection exists between the SH midlatitude circulations in the South Pacific and the structure of the circulation system comprised of the tropical Atlantic and West African monsoon. This connection is most pronounced during periods of significant wave activity in the South Pacific, which contributes to eddy growth in the South Atlantic. In addition to the SH influences, weaker, yet significant, connections to the NH were also identified. These connections are most pronounced when eddy activity in the North American region is enhanced.

Based on these results, areas for future research should involve a study of the energetics of this system, specifically attempting to address the causes of the eddy growth in the southeastern Pacific. Included in this could be an analysis of the role of the unique topography of the region, which includes the Drake Passage, the narrowest oceanic gap between the Antarctica and other continents, high mountains to the north (the Andes), and possible intense low-level temperature contrasts induced by the Antarctic peninsula. Furthermore, the role of the strength and structure of the SH jet stream should be evaluated.

A valuable extension of this would be to evaluate the contribution the South American wave events make to the start of the summertime West African monsoon. Lack of sufficient rains in West Africa has led to much civil strife and loss of life. A better understanding of the atmospheric circulations in this region could be critical to future military operations.

Based on the links established between tropical Atlantic circulations and cyclogenesis in the SH midlatitudes over South America, an examination of the relationship of wave activity in the tropical Atlantic to cold surge events in South America should be pursued.

# APPENDIX

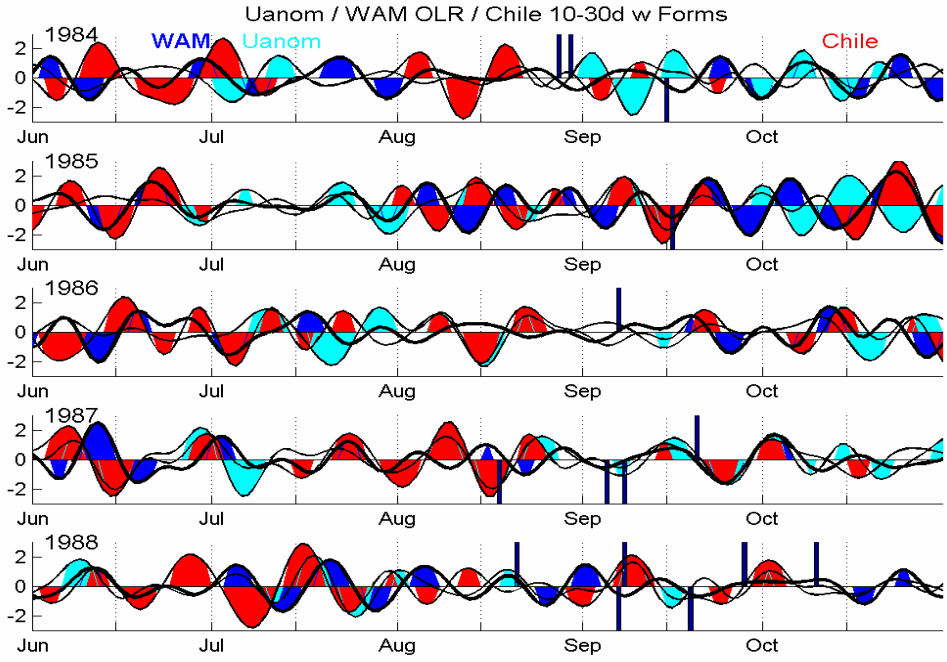


Figure A1 Daily time series from 1984-1988 of the zonal wind anomaly in the tropical Atlantic, OLRA over the WAM region, and 850-hPa streamfunction west of Chile (75°W-105°W, 45°S-60°S)

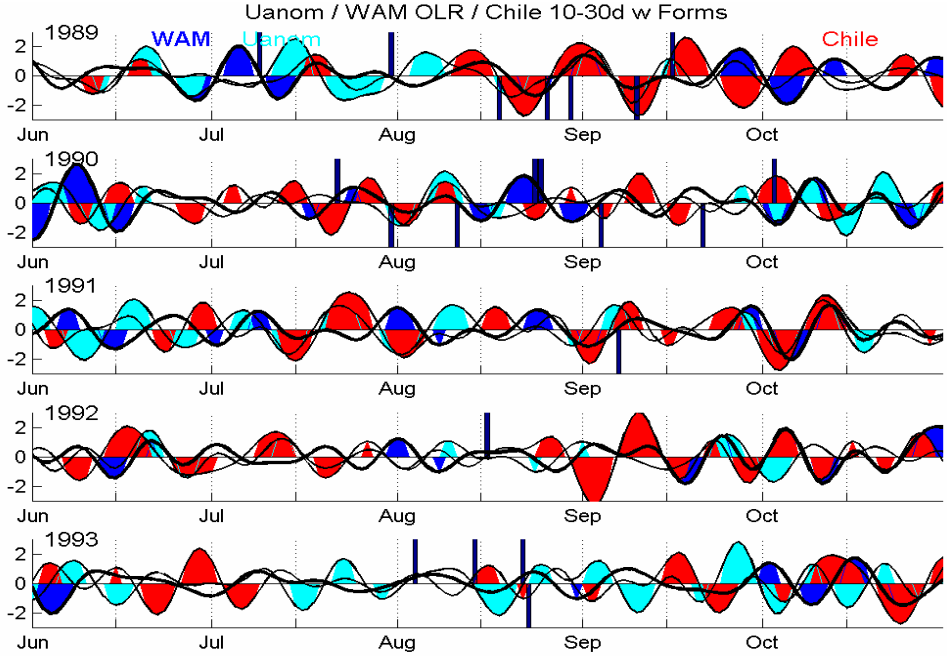


Figure A2 Daily time series from 1989-1993 of the zonal wind anomaly in the tropical Atlantic, OLRA over the WAM region, and 850-hPa streamfunction west of Chile (75°W-105°W, 45°S-60°S)

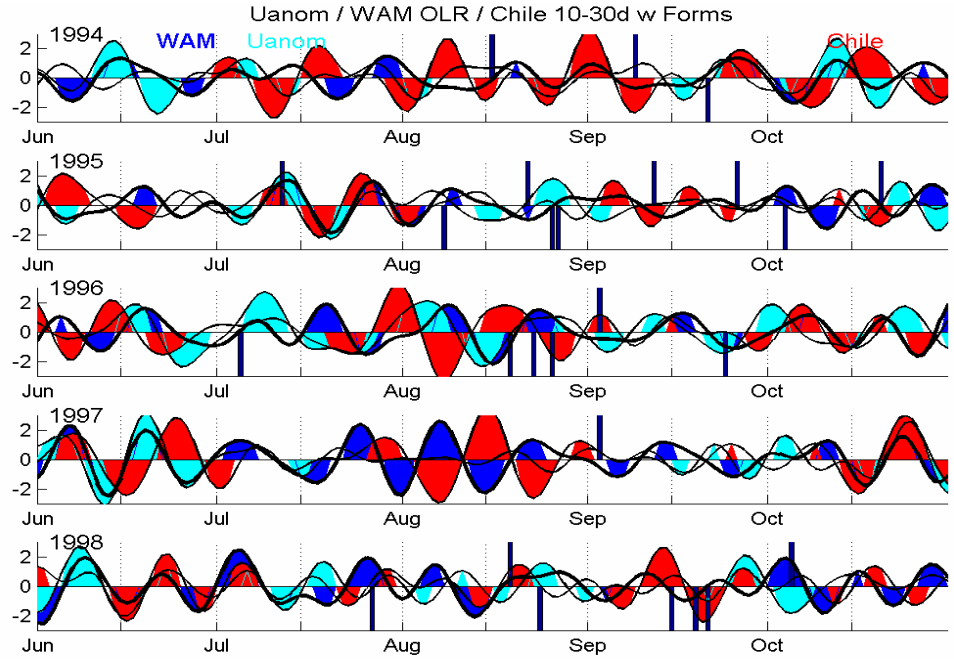


Figure A3 Daily time series from 1994-1998 of the zonal wind anomaly in the tropical Atlantic, OLRA over the WAM region, and 850-hPa streamfunction west of Chile (75°W-105°W, 45°S-60°S)

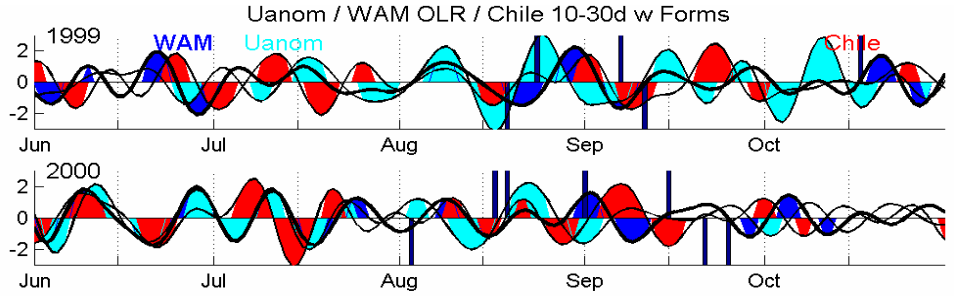


Figure A4 Daily time series from 1999 and 2000 of the zonal wind anomaly in the tropical Atlantic, OLRA over the WAM region, and 850-hPa streamfunction west of Chile (75°W-105°W, 45°S-60°S)

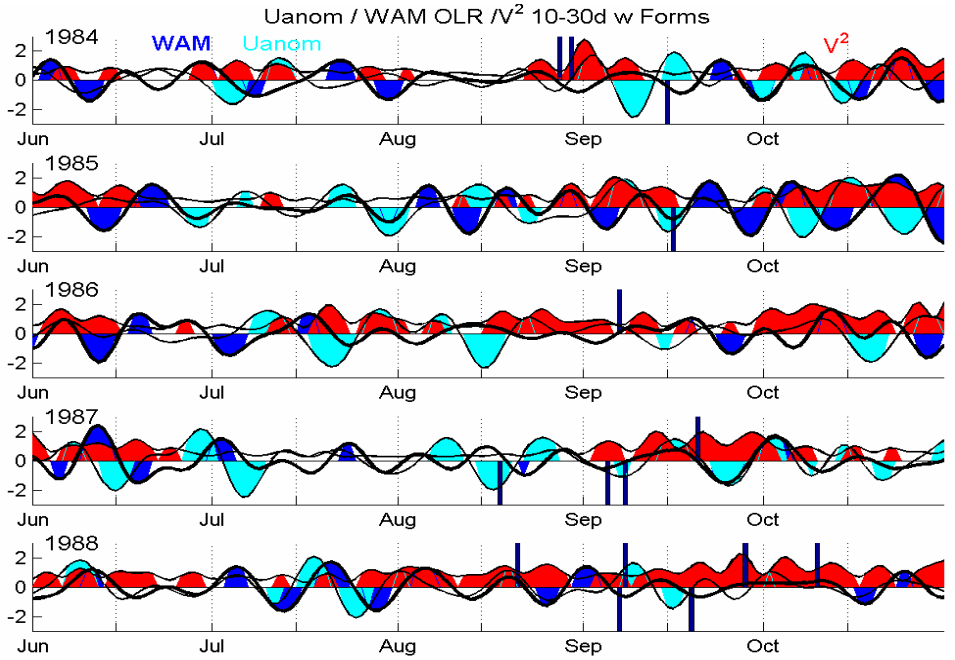


Figure A5 Daily time series from 1984-1988 of the zonal wind anomaly in the tropical Atlantic, OLRA over the WAM region, and squared value of the meridional component of the wind in the tropical Atlantic.

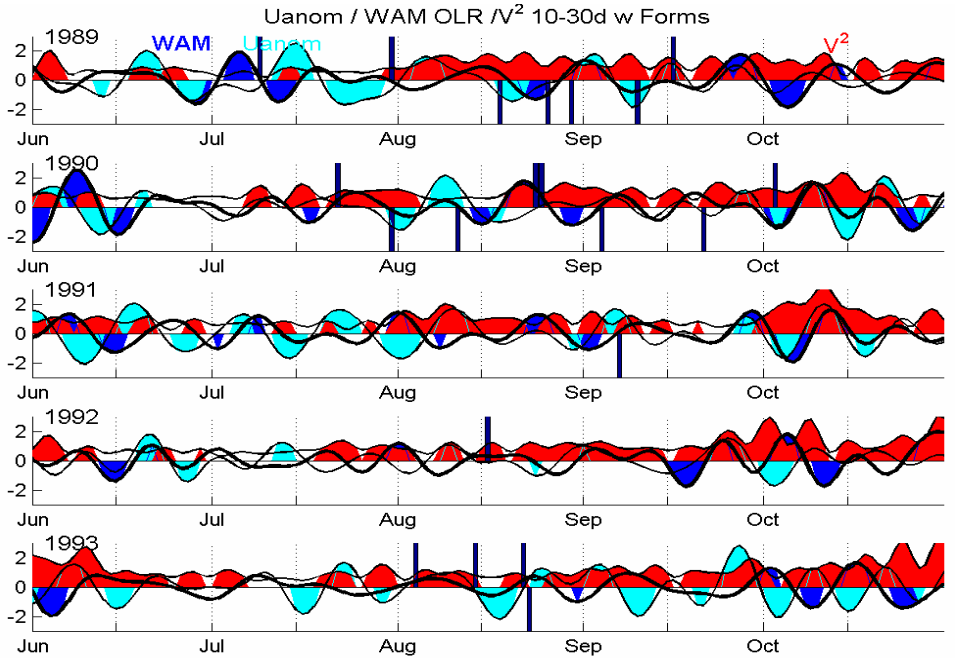


Figure A6 Daily time series from 1989-1993 of the zonal wind anomaly in the tropical Atlantic, OLRA over the WAM region, and squared value of the meridional component of the wind in the tropical Atlantic.

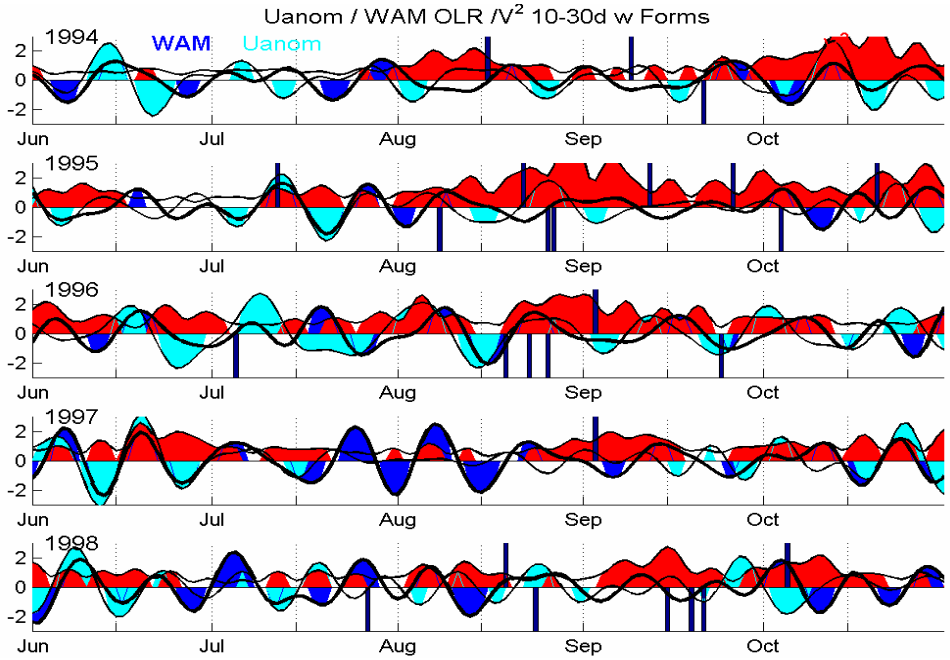


Figure A7 Daily time series from 1994-1998 of the zonal wind anomaly in the tropical Atlantic, OLRA over the WAM region, and squared value of the meridional component of the wind in the tropical Atlantic.

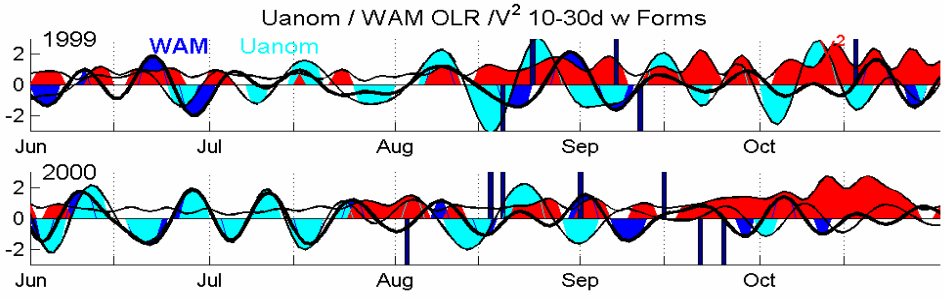


Figure A8 Daily time series from 1999-2000 of the zonal wind anomaly in the tropical Atlantic, OLRA over the WAM region, and squared value of the meridional component of the wind in the tropical Atlantic.

# LIST OF REFERENCES


Air Force Weather, 2004: AFW transformation: Strategic plan and vision FY2008-2032, U.S. Air Force distribution, 18 pp.

HQ United States Air Force, Director of Weather (HQ USAF/XOO–W), 2005: Air Force Weather Operations Functional Concept (Version 1.5). U.S. Air Force distribution, 25 pp.

Ambrizzi, T., B. J. Hoskins, and H. -H. Hsu, 1995: Rossby wave propagation and teleconnection patterns in the austral winter. *J. Atmos. Sci.,* **52,** 3661-3672.

Barnett, T. P. M., 2004: *The Pentagon's New Map: War and Peace in the Twenty-first Century*. G.P. Putnam's Sons, 435 pp.

Burton, K., 2005: Influence of the antarctic oscillation on intraseasonal variability of large-scale circulations over the western north pacific. M.S. Thesis, Dept. of Meteor., Naval Postgraduate School, 93 pp.

Delk, T. L., 2004: Intraseasonal, large-scale circulations and tropical cyclone activity over the western North Pacific during boreal summer. M.S. Thesis, Dept. of Meteor., Naval Postgraduate School, Monterey, CA, 76 pp.

DeMaria, M., J.A. Knaff, and B.H. Connell, 1999: A tropical cyclone genesis parameter for the tropical atlantic. *Wea. Forecasting,* **16,** 219-232.

Demmert, P., R. Whiton, K. Klein, F. Zawada, 2005: Value of weather services to the combatant commands: Volume I - Main Report and Appendices A & B. Air Force Weather Tech. Note AFWA/TN-05/001, 161 pp.

Duchon, C. E., 1979: Lanczos filtering in one and two dimensions. *J. Appl. Meteor.,* **18**, 1016-1022.

Grodsky, S. A., and J. A. Carton, 2001: Coupled land/atmosphere interactions in the west African monsoon. *Geophys. Res. Lett.,* **28,** 1503-1506

Hoskins, B.J., I. N. James, and G. H. White, 1983: The shape, propagation and mean-flow interaction of large-scale weather systems. *J. Atmos.Sci,*. **40,** 1595-1612.

——, and G. Y. Yang, 2000: The equatorial response to higher-latitude forcing. *J. Atmos. Sci.*, **57,** 1197-1213.

Kalnay, E., and Co-Authors, 1996: The NCEP/NCAR 40-year Re-analysis Project. *Bull. Amer. Meteor. Soc.,* **77,** 437-471.

Kiladis, G. N., and K.M. Weickmann, 1992a,: Circulation anomalies associated with tropical convection during northern winter. *Mon. Wea. Rev.,* **120,** 1900-1923.

——, and —— . 1992b: Extratropical forcing of tropical Pacific convection during northern winter. *Mon. Wea. Rev.,* **120,** 1924-1938.

——, and ——, 1997: Horizontal structure and seasonality of large-scale circulations associated with submonthly tropical convection. *Mon. Wea. Rev.,* **125,**, 1997-2013.

——, 1998: Observations of rossby waves linked to convection over the eastern tropical pacific. *J. Atmos. Sci.*, **55,** 321-335.

——, and K. C. Mo, 1998: Interannual and intraseasonal variability in the Southern Hemisphere. *Meteor. Monographs*, **27,** 307-336.

Landsea, C.W. and W.M. Gray, 1992: The strong correlation between western Sahelian monsoon rainfall and intense Atlantic hurricanes. *J. Climate*, **5,** 435-453.

Liebmann, B., and C. A. Smith, 1996: Description of a complete (interpolated) outgoing longwave radiation dataset. *Bull. Amer. Meteor. Soc.*, **77,** 1275-1277.

——, G. N. Kiladis, J. A. Marengo, T. Ambrizzi, and J.D. Glick, 1999: Submonthly convective variability over south America and the south atlantic convergence zone. *J. Climate*, **12,** 1877-1891.

Lorenz, E. N., 1956: Empirical Orthogonal Functions and statistical weather prediction. *Sci. Rep. 1,* Statistical Forecasting Project, Dept. of Meteor., MIT (NTIS AD 110268), 49 pp.

Madden, R. A., 1976: Estimates of the natural variability of time-averaged sea-level pressure. *Mon. Wea. Rev.,* **104,** 942-952.

McNielly, M., 2001: *Sun Tzu and the Art of Modern Warfare*. Oxford University Press, 304 pp.

——, and J. N. Paegle, 2001: The Pacific-South American modes and their downstream effects. *Int. J. Climatol.*, **21,** 1211-1229.

Richman, M. B., 1986: Rotation of principal components. *J. Climate*, **6,** 293-335.

Riehl, H., 1954: *Tropical Meteorology*. McGraw-Hill, 392 pp.

Satyamurty, P., Nobre, C. A., P. L. Silva Dias, 1998: Meteorology of the tropics: South America. *Meteor. Monographs,* **27,** 119-140.

Sultan, B., S. Janicot, and A. Dedhiou, 2003: The West African monsoon dynamics. Part I: documentation of intraseasonal variability. *J. Climate*, **16,** 3389-3406.

Thorncroft C. D., and K. Hodges, 2001: African easterly wave variability and its relationship to Atlantic tropical cyclone activity. *J. Climate*, **14**, 116-1179.

Torrence, C. and G. P. Compo, 1998: A Practical Guide to Wavelet Analysis. *Bull. Amer. Meteor. Soc.*, **79**, 61-78.

Wilks, D. S., 1995. *Statistical Methods in the Atmospheric Sciences.*, Academic Press, 467 pp.

THIS PAGE INTENTIONALLY LEFT BLANK

# INITIAL DISTRIBUTION LIST

1. Defense Technical Information Center
   Ft. Belvoir, Virginia

2. Dudley Knox Library
   Naval Postgraduate School
   Monterey, California

3. Professor Patrick Harr
   Naval Postgraduate School
   Monterey, California

4. Professor Tom Murphree
   Naval Postgraduate School
   Monterey, California

5. Professor Russell Elsberry
   Naval Postgraduate School
   Monterey, California

6. Dr. M. Steven Tracton
   Office of Naval Research
   Arlington, Virginia

7. Eric S. Blake
   NOAA/NCEP/TPC/NHC
   Miami, Florida

8. Captain Ken Burton
   25th Operational Weather Squadron
   Davis Monthan AFB, Arizona

9. Captain Matthew J. Rosencrans
   25th Operational Weather Squadron
   Davis Monthan AFB, Arizona